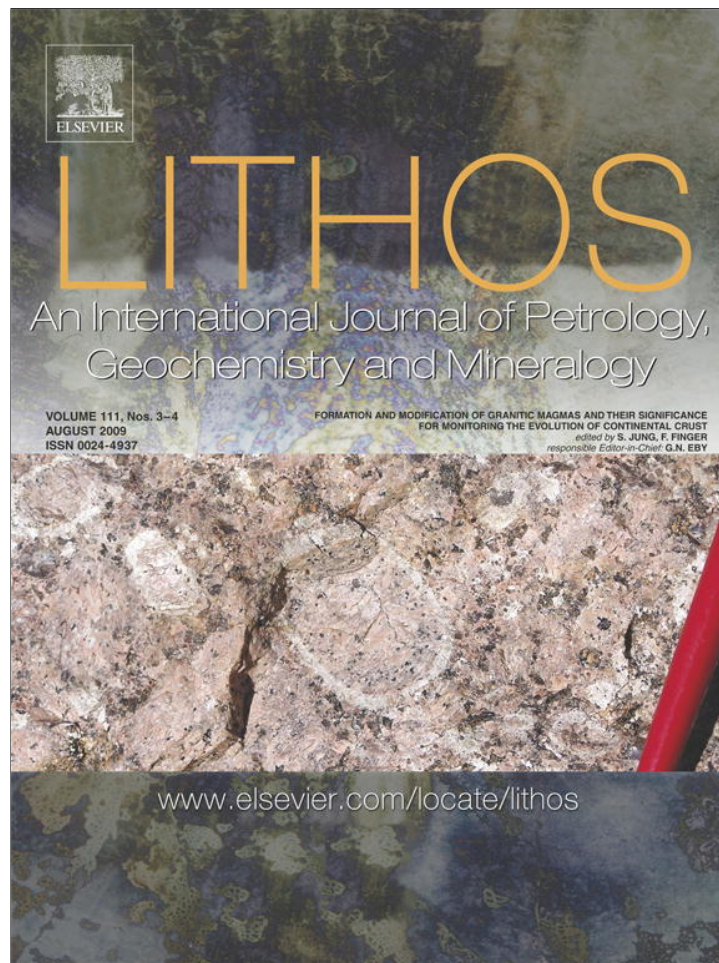


Provided for non-commercial research and education use.  
Not for reproduction, distribution or commercial use.



This article appeared in a journal published by Elsevier. The attached copy is furnished to the author for internal non-commercial research and education use, including for instruction at the authors institution and sharing with colleagues.

Other uses, including reproduction and distribution, or selling or licensing copies, or posting to personal, institutional or third party websites are prohibited.

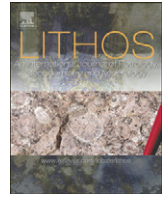
In most cases authors are permitted to post their version of the article (e.g. in Word or Tex form) to their personal website or institutional repository. Authors requiring further information regarding Elsevier's archiving and manuscript policies are encouraged to visit:

<http://www.elsevier.com/copyright>



Contents lists available at ScienceDirect

Lithos

journal homepage: [www.elsevier.com/locate/lithos](http://www.elsevier.com/locate/lithos)

# Genesis and emplacement of felsic Variscan plutons within a deep crustal lineation, the Penacova-Régua-Verín fault: An integrated geophysics and geochemical study (NW Iberian Peninsula)

H.C.B. Martins<sup>\*</sup>, H. Sant'Ovaia, F. Noronha

Department of Geology/Geology Centre, Faculty of Sciences, University of Porto, Rua do Campo Alegre, 4169-007 Porto, Portugal

## ARTICLE INFO

## Article history:

Received 29 February 2008

Accepted 17 October 2008

Available online 5 November 2008

## Keywords:

Variscan granites

I-type

Geophysics

Isotopic data

Emplacement

## ABSTRACT

Multidisciplinary studies integrating, U–Pb geochronology, whole-rock geochemical data, isotope geochemistry, anisotropy of magnetic susceptibility (AMS) studies and gravimetry were carried out on the Vila Pouca de Aguiar and the Águas Frias-Chaves porphyritic biotite granite plutons. Both plutons occur independently in a distance of about 20 km. The Vila Pouca de Aguiar and Águas Frias-Chaves plutons are examples of late to post-orogenic felsic Variscan granites in northern Portugal (NW Iberian Peninsula). The U–Pb zircon analyses yield a consistent age of  $299 \pm 3$  Ma which is considered to be the emplacement age of the two plutons. These granites are weakly peraluminous, show high HREE and Y (and low P) contents which are consistent with them being I-type. This is also supported by their weakly evolved isotopic compositions,  $^{87}\text{Sr}/^{86}\text{Sr}_i = 0.7044\text{--}0.7077$  and  $\epsilon\text{Nd} = -2.0$  to  $-2.6$ , as well as by the whole rock oxygen isotope ( $\delta^{18}\text{O}$  VSMOW) ranging from  $+9.7\%$  to  $+11.0\%$ . The emplacement of granite magma took place after the third Variscan deformation phase ( $D_3$ ) in an extensional tectonic regime, large scale uplift and crustal thinning. The integration of different data suggests that both plutons have the same feeding zone aligned within the Penacova-Régua-Verin fault (PRVF) and that both have the same structure which is related to late Variscan phases. The thicker shape for the Águas Frias-Chaves pluton comparing to that of the Vila Pouca de Aguiar pluton is compatible with different depths of PRVF sectors. The available data led us to propose a model of partial melting of a meta-igneous lower crustal source rather than an open-system of mantle–crust interaction. The interaction between the continental crust and invading mafic magmas could have been limited to mere heat transfer and, perhaps, local intermingling.

© 2008 Elsevier B.V. All rights reserved.

## 1. Introduction

The Variscan orogeny, a major event in the tectonic evolution of Western Europe, is currently explained by an obduction–collision orogenic model (Ribeiro et al., 1990; Matte, 1991; Dias and Ribeiro, 1995). In NW of the Iberian Peninsula, three main ductile deformation phases have been identified in this part of the Variscan belt (Ribeiro, 1974; Noronha et al., 1979; Ribeiro et al., 1990). The last ductile deformation phase ( $D_3$ ), Namurian–Westphalian in age, is followed by a brittle deformation phase (post- $D_3$ ), late Carboniferous to Permian in age which is characterised by a set of conjugate strike slip faults (NNW-dextral and NNE-sinistral), pointing to a late-Variscan main compression around N–S (Ribeiro, 1974; Arthaud and Matte, 1975). The  $D_3$  and the post- $D_3$  deformation phases are related to the post-thickening extensional tectonic regime (Lagarde et al., 1992; Dias and Ribeiro, 1995). During this post-collisional stage a continuous magmatic activity (mainly granitic) took place in the Central Iberian Zone and consequently in Northern Portugal. Based on several

geological data and U–Pb emplacement ages related to this third Variscan phase  $D_3$  (Ferreira et al., 1987; Dias et al., 1998; Martins, 1998), the post-collisional granites were divided into the following groups: synorogenic (sin- late- and late to post- $D_3$ ; 320–300 Ma) and late to post-orogenic (post- $D_3$ ; 299–290 Ma). The emplacement of the Vila Pouca de Aguiar and the Águas Frias-Chaves granite plutons, located in the Central Iberian Zone, Northern Portugal, (Farias et al., 1987), was controlled by the late brittle deformation phase, post- $D_3$  (Martins, 1998). The Penacova-Régua-Verin fault (PRVF) is one of the late Variscan deep crustal lineations, which belongs to the NNE–SSW trending brittle system that crosscuts the whole of Northern Portugal. The PRVF was nucleated on  $D_3$  and reactivated latter as a sinistral strike-slip fault with transtensional component. The granites presented in this paper are spatially related with this late strike slip fault, PRVF, and belong to the group of late to post-orogenic (post- $D_3$ ) granites. This fault, still tectonically active (Cabral, 1995), and in its NE branch presents several  $\text{CO}_2$  rich thermal water springs.

Multidisciplinary studies were carried out in order to compare structural and genetic features of the Vila Pouca de Aguiar and the Águas Frias-Chaves plutons and to point out the relation with PRVF. The aim of this work is to characterize the shape of pluton at depth, by

<sup>\*</sup> Corresponding author. Tel.: +351 22 0402461; fax: +351 22 0402490.  
E-mail address: [hbrites@fc.up.pt](mailto:hbrites@fc.up.pt) (H.C.B. Martins).

geophysical measurements, to investigate the age of emplacement and discuss the potential source materials, by major and trace elements geochemistry and isotope data, from representative post-D<sub>3</sub> Variscan plutons in northern Portugal.

## 2. Geological setting

The most common Portuguese Variscan granitoids in the Central Iberian Zone are biotite granodiorites and monzogranites and were emplaced during the post-collisional stage of Variscan orogeny. In the Vila Pouca de Aguiar and the Águas Frias-Chaves plutons, biotite

granites are the main variety and a detailed petrographic characterisation of these granites is present in Almeida et al. (2002).

The Vila Pouca de Aguiar and the Águas Frias-Chaves porphyritic biotite granite plutons are separated ca 20 km one from the other in independent outcrops and were emplaced into the major Régua-Verin fault, which belongs to the post-D<sub>3</sub> NNE-trending fault system (Fig. 1). The Águas Frias-Chaves granite pluton is a small body, more or less regular in outcrop, which occupies an area of 30 km<sup>2</sup> and it is composed of a marginal porphyritic biotite-rich coarse-medium grained granite, the Águas Frias granite (AFG), and by a central two-mica medium-grained granite, the S<sup>to</sup> António de Monforte granite

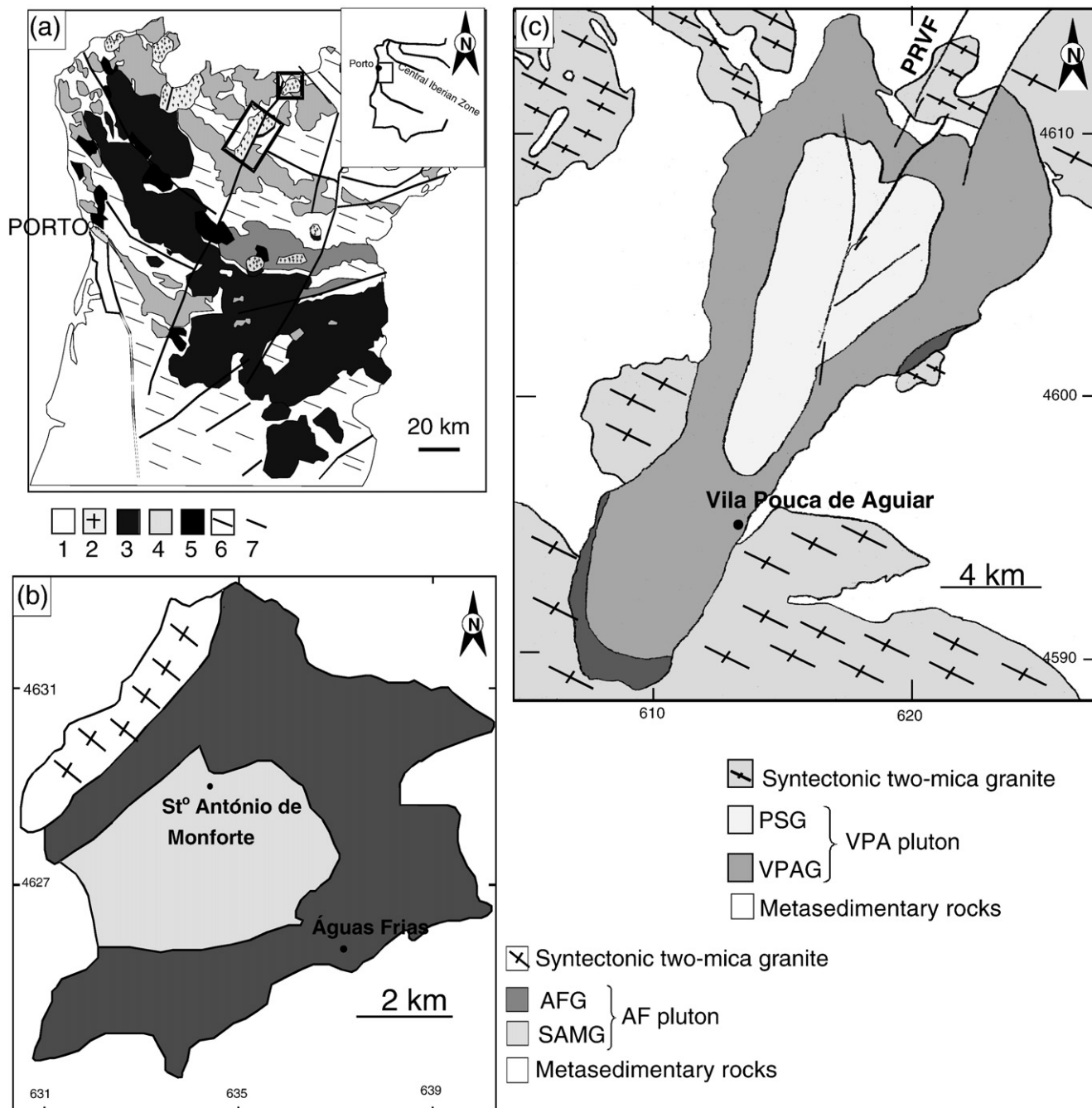


**Fig. 1.** (a) Geological distribution of Variscan syn to post-orogenic granitoids in Central Iberian Zone. 1. Post Palaeozoic; 2. Post-orogenic biotite granites; 3. Late-orogenic biotite granites; 4. Synorogenic two-mica granites; 5. Synorogenic biotite granites; 6. Metasedimentary rocks; 7. Faults. Inserted rectangles: studied plutons. (b and c) Sketch maps of the Águas Frias-Chaves and the Vila Pouca de Aguiar plutons. Geographical coordinates: UTM kilometric system. PSG: Pedras Salgadas Granite; VPAG: Vila Pouca de Aguiar Granite; AFG: Águas Frias granite; SAMG: S<sup>to</sup> António de Monforte granite. PRVF: Penacova- Régua-Verin Fault.

(SAMG) in which sampling is very difficult to obtain due to the scarcity of outcrops and weathering effects. The Vila Pouca de Aguiar pluton (ca 200 km<sup>2</sup>), has a NNE–SSW elongated shape, is a composite pluton with two main different biotitic granite facies: a peripheral biotite-rich granite, the Vila Pouca de Aguiar granite (VPAG) and a central biotite granite, the Pedras Salgadas granite (PSG). These granites define a more or less concentric zoning and the field relationships suggest a nearly synchronous magmatic emplacement.

The VPAG and AFG are medium- to coarse-grained granites characterized by a relative abundance of biotite and by a porphyritic texture composed of abundant light coloured K-feldspar megacrysts. The PSG is a homogeneous granite, also porphyritic, but more leucocratic than VPAG and AFG, and shows globular quartz in a medium- to fine-grained groundmass and relatively scarce K-feldspar megacrysts not larger than 2.5 cm. Both plutons are intruded into two-mica peraluminous granites ascribed to the D<sub>3</sub> Variscan event, and Upper Ordovician to Lower Devonian metasedimentary sequence of the “Peritranmontano” Domain (Ribeiro, 1974; Ribeiro, 1998; Ribeiro et al., 2004) characterised by D<sub>3</sub> N120° trending folds with subhorizontal axes and subvertical axial planar foliation (Ribeiro et al., 1990). The contacts are sharp, intrusive and discordant in relation to the general trending of the earlier Variscan structures which allow us to consider that the two plutons are late to post-orogenic or post-D<sub>3</sub>. These granites produced a metamorphic contact aureole (1 km width) with the assemblage quartz + K-feldspar + muscovite + cordierite ± andalusite (Brink, 1960; Ribeiro, 1998), indicating a shallow crustal emplacement level. Scarce rounded microgranular mafic enclaves of granodioritic or more rarely tonalitic composition, varying in size from 10 to 20 cm, are also observed specially in the VPAG (Neiva and Gomes, 1991).

The three granites are monzogranites in composition and they contain 30 to 32% modal quartz, 20 to 24% perthitic K-feldspar (orthoclase and microcline) and 37 to 42% plagioclase with normal zoning, oligoclase-andesine in the VPAG + AFG and albite-oligoclase in the PSG. Biotite (modal average of 5% in PSG and 9% in VPAG + AFG) is present as the only ferromagnesian phase. Accessory minerals include zircon, apatite, allanite, xenotime, ilmenite, sphene and rare monazite in PSG; some muscovite and rare cordierite are present in the AFG.

Although the AMS and the gravimetry studies were carried out on the two plutons as a whole, the geochemical data presented corresponds only to the main biotitic granitic facies (VPAG, PSG and AFG).

### 3. Analytical methods

#### 3.1. Geophysics

##### 3.1.1. Anisotropy of magnetic susceptibility

The AMS study was carried out to acquire a complete data set of the fabrics of the studied granites. At each site, four oriented cores (25 mm in diameter and 60 to 70 mm in length) were collected, each core being then sawed in two (eventually three) 22 mm long specimens. At least eight specimens per station were available for magnetic measurements. A total of 943 rock-cylinders were prepared for magnetic measurements for the Vila Pouca de Aguiar pluton. In the Águas Frias-Chaves pluton, the sampling grid is less dense and 125 rock-cylinders were measured. Measurements were performed using a KLY-3 Kappabridge susceptometer ( $\pm 3.8 \times 10^{-4}$  T; 920 Hz) (in “Laboratoire des Mécanismes et Transferts en Géologie” da Universidade Paul Sabatier de Toulouse) and in a KLY-4 S model in the Geology Centre, Department of Geology, Faculty of Sciences (Porto University). A sequence of several measurements along different orientations of each specimen allowed computing orientation and magnitude of the three main axes  $k_1 \geq k_2 \geq k_3$  of the anisotropy of magnetic susceptibility ellipsoid. With ExAMS program of Saint Blanquant (Unpublished) the mean susceptibility  $K_m$  of each site which is the mean of the six individual arithmetic means  $k_1 + k_2 + k_3 / 3$  was calculated. The three axes  $K_1 \geq K_2 \geq K_3$ , were also calculated, which are the vectorial means of

the  $k_1 \geq k_2 \geq k_3$  axes of the eight specimens.  $K_1$ , the long axis of the mean ellipsoid, is the magnetic lineation of the site and  $K_3$ , the short axis, is the normal to the magnetic foliation.  $P$ , the magnetic anisotropy ratio, corresponds to  $K_1/K_3$ . We have used in this study the parameter  $P_{para}\% = ((K_1 - D)/K_3 - D) - 1 \times 100$  and  $D (= -1.4 \times 10^{-5}$  SI), the diamagnetic component carried by the quartz and feldspars (Rochette, 1987). This parameter  $P_{para}\%$  is more convenient for the rocks displaying a low susceptibility from which it is necessary to subtract  $D$  which is constant and isotropic (Bouchez et al., 1987).

##### 3.1.2. Gravimetry

Amongst the geophysical tools applied to granite bodies, gravimetry measurements are best suited to investigate the shape of the plutons at depth. Through the inversion of gravity data, which is particularly sensitive to density contrasts, the shape at depth of the pluton, and depth of its floor, may be obtained with good confidence. The understanding of the 3 dimensional shapes of the granite bodies and of their floor's depth can be used to find the feeder zones of the plutons. This study deals with the characterization of 3 dimensional shapes of the Vila Pouca de Aguiar and the Águas Frias-Chaves plutons, using the interpretation of the gravity data and the modelling of the residual anomaly obtained.

In the Águas Frias-Chaves pluton gravity measurements were performed over 3649 closely spaced stations homogeneously distributed within an area of 379 km<sup>2</sup>, between the meridians 620 and 641 km and the parallels 4615 and 4632 km of the U.T.M. Kilometric System. In the Vila Pouca de Aguiar pluton 2027 measurements, were performed, corresponding to an area of 825 km<sup>2</sup>, between the meridians 605 and 630 km and the parallels 4586 and 4619 km of the U.T.M. Kilometric System. The raw gravity data were obtained with a gravimeter Lacoste and Romberg, G model, with a precision of  $\pm 0.01$  mGal and with temperature and pressure compensation. Elevations were determined using a precise ( $\pm 1$  m) baro-altimeter that was calibrated several times a day. The treatment of raw gravity data was comprised of several stages: gravimetric corrections, subtraction of the regional effect and modelling (inversion techniques). In a gravity survey, several effects are produced by sources, which are not of direct geological interest for the purpose of this study. Once these effects are removed by correcting the raw data to a datum (topography, elevation, latitude) and also from the tidal and instrumentation variations, the Bouguer anomaly values are determined. With these values, a grid can be computed and a Bouguer anomaly map is drawn. The combination of the isovalue contour line gradient of the Bouguer anomaly map and geological knowledge yields a first interpretation for the geometry of the granite body.

Our raw gravity data were corrected for the intrinsic constant of the apparatus and tidal effects and also for the usual topography, latitude and elevation corrections. The Bouguer correction was performed assuming a density of 2.70 and was interpolated by kriging along a one-kilometer sided grid. The residual anomaly for each one of the plutons was calculated from the Bouguer anomaly map by subtracting the regional gravity trend, which was modelled by a polynomial adjustment. According to Vigneresse (1990), the convenient residual anomaly map is obtained when the zero contour level of this map best outlines the contour of the granite body.

The residual anomaly was inverted using an iterative procedure. Among the several possible inversion methods, our modelling was performed using the 3-D iterative procedure derived from Cordell and Henderson (1968) adapted to small-scale gravimetric investigations by Vigneresse (1990). In this process (Ameglio et al., 1997), the source was roughly modelled by small prisms each having a constant density and a progressive adjustment was performed until the calculated gravity field fitted the observed data. A map of surface densities for the main granite types of the two plutons and surrounding rocks, have been incorporated in the computation, in order to better constrain the nominal densities of the prisms. Data inversion was also tested with

**Table 1**  
Major (wt.%), trace and rare earth (ppm) elements data of samples from Vila Pouca de Aguiar granite (VPAG), Pedras Salgadas granite (PSG) and Águas Frias granite (AFG), northern Portugal.

Samples	VPAG										PSG										AFG															
	74-3	74-12	74-15	74-16	74-9	74-5	74-20	74-4B	46-2	61-13	61-6A	61-6B	60-14	60-15	60-16	60-11	60-12	60-17	60-13	60-10	60-18	60-19	61-6	74-8	74-7	74-11	60-1	60-2	34-4	CV1	CV2	CV-8	CV-11	CV-13		
SiO <sub>2</sub>	70.72	71.52	72.24	71.96	72.89	71.72	70.65	71.84	71.77	71.36	70.74	70.91	71.04	72.35	70.65	70.47	71.18	73.77	73.62	74.24	73.00	74.47	74.40	74.12	73.56	73.95	72.40	73.72	72.77	73.11	72.19	71.96	72.71	73.85		
TiO <sub>2</sub>	0.39	0.35	0.31	0.4	0.3	0.3	0.43	0.38	0.34	0.37	0.36	0.36	0.39	0.34	0.36	0.32	0.36	0.17	0.15	0.19	0.12	0.15	0.17	0.18	0.24	0.17	0.20	0.34	0.28	0.32	0.31	0.30	0.29			
Al <sub>2</sub> O <sub>3</sub>	14.51	14.57	13.35	13.66	13.73	13.59	14.11	13.46	13.56	14.07	14.36	14.11	14.03	13.51	13.56	14.41	13.83	13.53	13.38	13.35	13.57	13.33	13.48	13.65	14.08	13.90	13.87	13.98	13.82	13.61	14.07	13.90	13.84	13.31		
Fe <sub>2</sub> O <sub>3t</sub>	3.08	2.47	2.22	2.62	2.09	2.8	3.22	2.97	2.72	2.9	2.74	2.94	2.9	2.72	2.87	2.59	2.95	1.62	1.77	1.62	1.76	1.41	1.62	1.56	1.45	1.51	1.63	1.55	2.48	2.26	2.30	2.24	2.27	2.16		
MnO	0.06	0.06	0.05	0.06	0.06	0.05	0.04	0.04	0.04	0.04	0.04	0.04	0.04	0.05	0.04	0.04	0.03	0.04	0.03	0.04	0.03	0.03	0.05	0.07	0.08	0.05	0.06	0.05	0.05	0.05	0.05	0.05	0.05	0.05		
MgO	0.79	0.63	0.51	0.64	0.61	0.49	0.79	0.7	0.64	0.71	0.65	0.68	0.69	0.61	0.65	0.58	0.63	0.25	0.32	0.26	0.32	0.25	0.26	0.42	0.32	0.33	0.40	0.28	0.70	0.62	0.69	0.65	0.64	0.60		
CaO	1.99	1.63	1.54	1.75	1.5	1.71	1.93	1.62	1.67	1.79	1.9	1.75	1.83	1.67	1.79	1.61	1.58	1.18	0.86	1.03	1.18	0.83	1.04	0.88	1.12	0.98	1.05	1.26	1.51	1.65	1.80	1.66	1.63	1.56		
Na <sub>2</sub> O	3.68	3.7	3.54	3.5	3.62	3.52	3.5	3.34	3.47	3.54	3.66	3.58	3.47	3.45	3.47	3.58	3.32	3.50	3.45	3.54	3.52	3.55	3.45	3.52	3.45	3.33	3.61	3.38	3.49	3.53	3.61	3.54	3.50	3.39		
K <sub>2</sub> O	4.41	4.62	4.47	4.2	4.25	4.26	4.24	4.25	4.3	4.26	4.26	4.36	4.33	4.2	3.95	4.82	4.54	4.59	4.67	4.55	4.52	4.67	4.47	4.91	4.64	4.79	4.61	4.64	4.08	4.05	4.21	4.09	4.01	3.96		
P <sub>2</sub> O <sub>5</sub>	0.12	0.06	0.14	0.16	0.07	0.11	0.13	0.11	0.11	0.15	0.13	0.12	0.13	0.1	0.11	0.12	0.13	0.06	0.07	0.06	0.07	0.05	0.07	0.04	0.05	0.10	0.02	0.05	0.15	0.13	0.14	0.15	0.15	0.13		
LOI	0.62	0.67	0.61	0.83	0.82	0.9	0.77	1.09	1.18	0.63	0.93	0.93	0.95	0.81	1.23	1.04	1.23	1.10	1.15	1.02	1.12	1.10	0.85	0.76	0.76	0.90	0.76	0.61	0.80	0.64	0.54	0.59	0.69	0.76		
Total	100.4	100.3	98.98	99.78	99.94	99.45	99.81	99.8	99.8	99.82	99.77	99.78	99.8	99.8	98.69	99.58	99.79	99.79	99.50	99.85	99.29	99.81	99.82	100.1	99.61	100.1	98.57	99.66	100.19	99.94	99.93	99.14	99.80	100.07		
Ba	330	401	362	331	266	264	375	332	267	339	344	373	345	275	284	416	453	302	289	265	295	271	277	272	250	200	330	225	288	267	308	319	300	257		
Rb	233	234	251	247	214	245	236	243	263	222	242	222	232	226	222	245	221	225	254	276	237	273	237	277	278	312	237	287	228	237	241	227	231	216		
Sr	69	124	113	101	102	36	108	90	86	98	103	100	103	83	88	100	103	69	71	65	70	58	66	44	75	60	85	75	89	82	98	103	90	82		
Cs	23.8	17.5	18.1	-	13.8	-	18.9	18.8	19.4	-	-	-	-	-	18.6	26.2	17.0	35.2	18.0	17.7	23.9	22.6	16.0	19.0	22.0	-	19.9	20.2	-	19.2	24.5	22.1	19.2	17.8	20.6	23.8
Co	5.00	3.90	3.40	-	36.50	-	5.23	4.49	4.33	4.00	4.22	4.31	4.64	4.27	4.26	3.94	4.00	1.89	1.96	2.04	2.00	1.60	1.70	-	1.00	1.00	-	1.20	4.21	3.53	3.96	3.84	3.00	3.00		
Cr	31.0	29.0	33.0	-	29.0	-	72.7	65.0	87.3	76.0	82.3	99.0	48.9	79.4	73.1	62.8	85.5	72.7	74.0	75.8	54.0	68.8	48.0	-	26.0	28.0	-	32.0	56.1	114.0	47.5	51.8	49.0	41.0		
Zn	54.0	46.0	47.0	-	13.0	-	54.8	51.6	46.3	46.0	42.6	58.6	51.4	44.8	49.5	46.0	55.0	33.3	28.9	35.0	33.0	34.0	37.9	-	36.0	42.0	-	27.0	63.5	36.0	61.6	65.2	53.0	36.0		
Sn	15.00	2.00	13.00	-	20.00	-	11.30	12.00	13.60	-	-	-	-	-	10.70	14.00	15.10	10.90	12.00	10.60	11.00	17.00	9.96	15.90	18.00	-	21.00	57.00	-	26.00	13.05	12.66	12.75	13.44	13.00	12.00
W	6.80	2.10	0.80	-	-	-	2.43	2.00	2.29	-	-	-	1.43	1.90	3.15	6.92	5.00	2.84	4.89	2.80	2.06	2.49	3.42	-	1.50	1.60	-	3.60	1.81	1.13	-	-	-	-		
Nb	16.30	15.70	15.70	-	14.50	-	14.20	14.90	14.40	13.60	-	-	-	-	13.30	13.60	14.30	12.80	13.80	12.10	13.00	14.00	13.00	13.00	14.00	-	15.20	15.90	-	15.60	17.89	14.70	15.94	16.29	17.00	15.00
Zr	169	162	153	-	126	-	196	189	157	173	170	172	155	150	158	148	189	99	110	108	106	87.8	100	-	96	98	-	97	147	122	144	136	134	117		
Ga	24.00	24.00	23.00	-	24.00	-	22.00	21.70	21.30	20.00	21.70	21.30	20.90	19.70	20.00	22.00	21.80	18.00	19.00	20.70	19.00	19.70	19.00	-	25.00	26.00	-	27.00	20.93	18.65	20.02	21.02	19.00	18.00		
Th	16.15	19.82	18.72	-	17.60	-	18.00	20.60	21.60	20.80	19.00	24.20	15.00	16.50	12.90	17.00	26.50	21.00	21.50	20.70	22.90	19.40	19.00	-	20.69	20.84	-	23.26	19.07	15.63	17.65	18.08	17.00	14.50		
Y	36.00	37.00	38.00	-	36.00	-	38.00	41.80	48.40	39.90	41.30	40.70	36.00	38.40	37.30	26.60	40.80	33.00	40.00	37.00	39.80	43.60	27.00	-	35.00	40.00	-	35.00	32.93	29.82	32.10	30.48	34.00	30.00		
V	30.00	22.00	20.00	-	19.00	-	35.60	29.60	27.70	31.60	28.80	28.50	29.00	26.40	26.20	24.00	26.00	10.80	13.70	11.00	12.90	10.00	10.70	-	10.00	9.00	-	11.00	-	-	-	-	-	-		
Be	6.00	5.00	6.00	-	5.00	-	6.57	5.83	7.77	5.69	6.38	4.07	5.80	6.98	7.00	6.79	5.00	5.15	5.57	8.45	5.74	8.78	6.00	-	6.00	8.00	-	10.00	7.00	6.00	6.00	5.00	5.00	5.00		
U	5.51	6.81	9.29	-	6.69	-	8.35	8.47	9.07	-	-	-	7.51	10.70	5.08	6.85	8.53	7.86	12.60	12.50	7.46	10.00	13.50	-	4.43	4.83	-	12.53	5.78	12.40	16.64	5.93	4.80	5.80		
Hf	5.10	5.10	4.60	-	4.10	-	-	-	-	-	-	-	-	-	-	-	-	-	-	-	-	-	-	-	3.60	3.60	-	3.70	4.87	4.15	4.77	4.17	4.40	3.90		
La	28.77	-	27.32	-	-	-	32.72	30.53	26.08	36.02	30.77	33.10	25.84	26.05	27.72	33.59	39.99	27.81	27.92	26.24	26.11	25.46	24.40	-	-	31.50	-	33.10	24.16	27.47	31.39	30.90	25.60			
Ce	66.48	-	66.23	-	-	-	70.23	65.51	57.05	73.04	66.47	69.21	54.85	55.33	59.97	71.38	83.18	57.57	56.23	56.34	55.40	52.85	48.24	-	-	70.50	-	67.78	50.60	57.73	64.03	65.20	54.40			
Nd	27.47	-	25.12	-	-	-	31.75	30.43	27.68	32.08	30.07	31.58	24.61	28.04	27.60	29.69	37.40	23.63	23.64	23.68	25.52	22.67	21.07	-	-	25.21	-	28.64	22.55	25.51	27.08	27.80	23.40			
Sm	6.45	-	6.05	-	-	-	7.42	7.15	6.65	7.43	6.98	6.88	6.23	7.10	6.54	5.81	7.59	5.62	5.39	5.66	6.12	5.64	4.88	-	-	5.95	-	6.28	5.21	5.91	5.96	6.80	5.90			
Eu	1.04	-	0.94	-	-	-	1.03	0.81	0.77	0.74	0.81	0.74	0.80	0.89	0.78	0.77	0.88	0.54	0.50	0.58	0.70	0.47	0.55	-	-	0.72	-	0.64	0.56	0.67	0.68	0.65	0.55			
Gd	6.11	-	5.64	-	-	-	6.30	6.11	6.32	5.87	6.86	6.56	5.47	6.00	5.83	4.99	7.22	4.87	4.91	5.09	5.60	5.36	4.16	-	-	5.44	-	6.01	5.17	5.70	5.56	6.00	5.20			
Dy	5.91	-	5.68	-	-	-	6.42	6.63	7.22	6.21	6.46	6.29	5.89	6.63	6.23	4.37	6.34	5.59	5.75	5.61	6.56	6.59	4.68	-	-	5.50	-	5.96	5.23	5.68	5.46	6.00	5.20			
Er	3.28	-	3.26	-	-	-	3.29	3.72	4.53	3.50	3.90	3.83	3.23	3.89	3.72	2.28	3.65	3.33	3.50	3.42	3.97	4.10	2.66	-	-	3.12	-	3.41	3.02	3.23	3.05	3.60	3.30			
Yb	3.35	-	3.59	-	-	-	3.70	4.05	5.41	3.89	4.51	4.19	4.13	4.94	4.67	2.44	3.90	4.23	4.00	4.38	4.91	5.93	3.55	-	-											

respect to sensitivity of results to the density contrasts. A map of the calculated depth of the pluton floor was finally obtained. Densities were measured using the cylindrical specimens that were collected for the AMS study. Densities were determined with the pycnometer technique as described by Vigneresse and Cannat (1987): the cores were set under vacuum, impregnated by water and weighed, then slowly dried to avoid thermal cracking, and weighed again.

### 3.2. Geochemistry

#### 3.2.1. Whole rock geochemistry

Representative major- trace- and rare-earth element data of the three granites studied, the VPAG, the PSG and the AFG, are reported in Table 1. Whole-rock chemical compositions from the VPAG and the PSG were analysed by inductively coupled plasma emission spectrometry, ICP-AES, and ICP-MS, mass spectrometry using the method of Govindaraju and Mevelle (1987) at CRPG, Nancy, France. The precision of the analyses was about 1% for major elements and most trace elements. Some trace elements (W, U, Th, Ta and Hf) were analysed by neutron activation, INAA, (Hofmann, 1992). Major- trace- and rare-earth element compositions from the AFG were obtained by ICP-MS at Activation Laboratories (Canada). Precision and accuracy of ICP-MS analyses are commonly within 10%.

The validity and usefulness of any compositional data are crucially dependent upon the quality of the sample collected in the field, so thirty four representative samples, 12–15 kg each, were collected in outcrops and some quarries taking into account that all of them were as fresh and unweathered as possible.

#### 3.2.2. Sr–Nd isotopes

Thirteen samples were selected for Rb–Sr and nine of these for Sm–Nd isotopic analysis (Table 2). Rb–Sr and Sm–Nd isotopes from the VPAG and the PSG were analysed at CRPG, Nancy, France, using techniques described by Michard et al. (1985). The concentrations of Rb, Sr and Sm, Nd were determined by isotopic dilution and Rb isotopic ratios were measured using a Cameca TSN 206 mass spectrometer, while Sr, Sm and Nd isotopic ratios were measured with a Finnigan MAT 262 mass spectrometer. The  $^{87}\text{Sr}/^{86}\text{Sr}$  and  $^{143}\text{Nd}/^{144}\text{Nd}$  ratios were corrected for mass fractionation effects to  $^{86}\text{Sr}/^{88}\text{Sr} = 0.1194$  and  $^{146}\text{Nd}/^{144}\text{Nd} = 0.7219$  using NBS 987 Standard. The maximum uncertainties in  $^{87}\text{Rb}/^{86}\text{Sr}$  and  $^{147}\text{Sm}/^{144}\text{Nd}$  were 1.5% and 0.5% respectively, at the 95% confidence level ( $2\sigma$ ).

Measurements of Sr and Nd isotope values from the AFG (three samples) were carried out at the Laboratoire Magmas et Volcans,

Clermont-Ferrand (France). Chemical procedures for sample preparation are described in Pin et al. (1994) and Pin and Santos Zalduegui (1997). Sm and Nd concentrations were determined by isotope-dilution TIMS using a mixed  $^{149}\text{Sm}$ – $^{150}\text{Nd}$  tracer. The  $^{147}\text{Sm}/^{144}\text{Nd}$  values are precise to  $\pm 0.2\%$  at the 95% confidence level.  $^{143}\text{Nd}/^{144}\text{Nd}$  ratios were measured by TIMS in a ThermoFinnigan Triton instrument in static multicollection mode, and corrected for mass fractionation by normalization to  $^{146}\text{Nd}/^{144}\text{Nd} = 0.7219$ . The JNdi isotopic standard measured under the same conditions gave  $^{143}\text{Nd}/^{144}\text{Nd} = 0.512099(1)$ .  $^{87}\text{Sr}/^{86}\text{Sr}$  ratios were measured by TIMS using a modified VG54E instrument in static multicollection mode, and corrected for mass fractionation by normalization to  $^{86}\text{Sr}/^{88}\text{Sr} = 0.1194$ . The reported  $^{87}\text{Sr}/^{86}\text{Sr}$  ratios were adjusted to the NIST SRM 987 standard  $^{87}\text{Sr}/^{86}\text{Sr} = 0.710244(20)$ , at the 95% confidence level ( $2\sigma$ ).

In the calculations of  $\epsilon_{\text{Nd}}$ ,  $^{143}\text{Nd}/^{144}\text{Nd}_{\text{CHUR}} = 0.512638$  and  $^{147}\text{Sm}/^{144}\text{Nd}_{\text{CHUR}} = 0.1967$  (Jacobsen and Wasserburg, 1984) have been used. Regression lines on a  $^{87}\text{Sr}/^{86}\text{Sr}$  vs  $^{87}\text{Rb}/^{86}\text{Sr}$  plot have been calculated using the least-squares method as implemented in the Isoplot program (Ludwig, 2003).

#### 3.2.3. Oxygen isotope

Oxygen isotope data were performed on seven samples analysed for Sr and Nd isotopes at the Stable Isotopic Laboratory of Salamanca. Oxygen was extracted from rocks by laser fluorination techniques, quantitatively converted to  $\text{CO}_2$  by the reaction with a heated carbon rod and analyzed for  $^{18}\text{O}/^{16}\text{O}$  ratio with a dual inlet VG SIRA-II Mass Spectrometer. The analytical data are reported in the familiar  $\delta$ -notation referenced to SMOW. Two or more extractions were made on each sample; the reproducibility of isotopic analyses is  $\pm 0.1\%$ . NBS-28 yielded an average  $\delta^{18}\text{O}$  value of 9.5‰ VSMOW. The isotopic results, along with the calculated initial  $^{87}\text{Sr}/^{86}\text{Sr}$  and  $\epsilon_{\text{Nd}}$  values are given in Table 2.

#### 3.2.4. U–Pb dating

The U–Pb isotopic analyses were carried out also at CRPG, Nancy, France, using a conventional U–Pb method on multigrain zircon fractions. The zircons were recovered by crushing the sample and sieving, followed by heavy liquid and magnetic separations and finally hand picking. Four zircon fractions were selected according to their morphology, colour, and lack of inclusions, fractures and metamictisation. Some of these fractions were submitted to air-abrasion (Krogh, 1982) to eliminate the external zones of the crystal where Pb loss may have occurred. All zircon fractions were observed on a backscattered scanning electron microscopy (BSEM).

**Table 2**  
Sr, Nd and  $\delta^{18}\text{O}$  isotopic data selected from Vila Pouca de Aguiar granite (VPAG), Pedras Salgadas granite (VPAG), Pedras Salgadas granite (PSG) and Águas Frias granite (AFG), northern Portugal.

	Rb tot (ppm)	Sr tot (ppm)	$^{87}\text{Rb}/^{86}\text{Sr}$	$^{87}\text{Sr}/^{86}\text{Sr}$ $\pm (2\sigma)$	$^{87}\text{Sr}/^{86}\text{Sr}_i$ (299 Ma)	Nd (ppm)	Sm (ppm)	$^{147}\text{Sm}/^{144}\text{Nd}$	$^{143}\text{Nd}/^{144}\text{Nd}$ $\pm (2\sigma)$	$\epsilon_{\text{Nd}}$ (299 Ma)	$\delta^{18}\text{O}$ ‰
<b>VPAG</b>											
60-12 b	217.25	106.69	5.906	0.732084 (30)	0.7069	33.21	8.39	0.1529	0.512423 (8)	−2.6	10.3
60-16 b	202.09	91.00	6.444	0.734166 (41)	0.7067	–	–	–	–	–	–
46-2 b	261.65	86.52	8.779	0.744242 (22)	0.7069	24.31	5.8	0.1443	0.512410 (9)	−2.5	10.3
74-3 b	222.39	114.79	5.617	0.730929 (25)	0.7070	26.52	5.95	0.1357	0.512392 (12)	−2.5	–
74-12 b	232.19	99.33	6.781	0.735986 (29)	0.7071	–	–	–	–	–	–
<b>PSG</b>											
60-10 b	275.89	67.35	11909.000	0.755493 (24)	0.7048	20.56	5.05	0.1431	0.512435 (7)	−2.0	10.5
60-13	266.27	71.53	10814.000	0.750709 (25)	0.7047	21.33	4.87	0.1381	0.512423 (12)	−2.0	11.0
60-17	253.36	71.43	10302.000	0.748267 (20)	0.7044	–	–	–	–	–	–
60-19	290.98	58.58	14465.000	0.766501 (29)	0.7050	19.44	4.77	0.1484	0.512444 (7)	−2.0	10.3
74-8	272.49	109.6	7255.000	0.735876 (37)	0.7052	–	–	–	–	–	–
<b>AFG</b>											
34-4	228.46	88.63	7.437	0.73934(10)	0.7077	29.10	6.05	0.1257	0.512371(5)	−2.5	9.7
CV-2	241.49	97.65	7.135	0.737973(13)	0.7076	29.90	6.26	0.1265	0.512373(4)	−2.5	9.8
CV-13	215.95	82.01	7.645	0.740401(15)	0.7079	27.30	5.89	0.1303	0.51238(5)	−2.5	–

**Table 3**  
U–Pb isotopic data on zircon from late- to post-orogenic Vila Pouca de Aguiar granite (VPAG).

Fractions (shape)	Concentrations				Isotopic ratios			Apparent ages (Ma)		
	Weight (mg)	U Total (ppm)	Pb* (ppm)	<sup>206</sup> Pb/ <sup>204</sup> Pb	<sup>206</sup> Pb*/ <sup>238</sup> U 2σ(%)	<sup>207</sup> Pb*/ <sup>235</sup> U 2σ(%)	<sup>207</sup> Pb*/ <sup>206</sup> Pb* 2σ(%)	<sup>206</sup> Pb*/ <sup>238</sup> U 2σ	<sup>207</sup> Pb*/ <sup>235</sup> U 2σ	<sup>207</sup> Pb*/ <sup>206</sup> Pb* 2σ
74-20/A (Z) na (Needle)	0.26	1424	56.6	294	0.040655 ± 0.134	0.292862 ± 0.362	0.052245 ± 0.243	256.9 ± 0.3	260.8 ± 0.8	296 ± 6
74-20/B (Z) na (Flat)	0.25	2279	82.3	350	0.037278 ± 0.125	0.26829 ± 0.395	0.052198 ± 0.289	235.9 ± 0.3	241.3 ± 0.8	294 ± 7
74-20/C (Z) a (Short prisms)	0.12	1123.0	49.4	2092	0.045184 ± 0.093	0.325718 ± 0.189	0.052283 ± 0.985	284.9 ± 0.3	286.3 ± 0.5	298 ± 2
74-20/D (Z) a (Long prisms)	0.13	498.0	22.4	626	0.0453 ± 0.163	0.326624 ± 0.422	0.052294 ± 0.271	285.6 ± 0.5	287 ± 1.1	298 ± 4

a: fraction submitted to abrasion; na: fraction not submitted to abrasion; Pb\* radiogenic lead.

Chemical preparation of U and Pb analysis includes: (1) HNO<sub>3</sub> 3 N warm washing of the zircon; (2) HF digestion at 240 °C and HCl 3 N dissolution of the fluorides at 180 °C in a Teflon bomb (Parrish, 1987); (3) separation of Pb and U by elution on anionic resin of two aliquots (one with the addition of a mixed <sup>208</sup>Pb–<sup>235</sup>U spike) following Krogh (1973). Common Pb blanks varied from 30 and 80 pg during this study. The atomic ratios were corrected for initial common lead composition blanks (Stacey and Kramers, 1975) and mass fractionation using NBS 983 Standard. The U–Pb ages with 2σ errors were calculated using a version of Isoplot program (Ludwig, 2003). The decay constants used for age determinations are from Steiger and Jäger (1977). The U–Pb zircon analytical data are presented in Table 3.

## 4. Results

### 4.1. Geophysics

#### 4.1.1. Anisotropy of Magnetic Susceptibility (AMS)

In the Vila Pouca de Aguiar pluton, the susceptibility magnitudes rang from 40 to 220 × 10<sup>−6</sup> SI according to a well-defined zoning with an average value of 101.0 × 10<sup>−6</sup> SI (also see Sant’Ovaia et al., 2000). In the Águas Frias-Chaves pluton, the susceptibility range from 40.0 to 103.0 × 10<sup>−6</sup> SI with an average value of 80.7 × 10<sup>−6</sup> SI (Sant’Ovaia and Noronha, 2005a). Such low susceptibilities which characterize magnetite-free granites (see Rochette, 1987) are typical of paramagnetic granites (Bouchez, 1997). In the latter the iron is dominantly carried by the silicates, principally biotite in our case.

In both plutons magnetic susceptibility values characterize perfectly each one of the granite types: higher average values of 135.5 × 10<sup>−6</sup> SI and 89.2 × 10<sup>−6</sup> SI were found for the VPAG and the AFG respectively, and lower values of 67.8 and 42.2 × 10<sup>−6</sup> SI for the PSG and the SAMG. These values characterize the mineralogical difference between central facies and peripheral facies. Susceptibility is therefore directly correlated with the amount of biotite which increases from the centre to the periphery of the plutons (Martins et al., 2007). The anisotropy magnitudes are quite low, always lower than 2% for all the sampled sites: 1.4% for the Vila Pouca de Aguiar pluton and 1.6% for the Águas Frias-Chaves pluton. In VPAG pluton the highest anisotropy values are correlated with the least magnetic granites; in Águas Frias-Chaves pluton there are no differences between central and peripheral granites.

AMS fabric patterns are very regular throughout the plutons. In the Vila Pouca de Aguiar pluton, magnetic foliations have moderate outward dips (the dip average is 34°) with strikes more or less parallel to the pluton elongation and are concordant for both granites. Magnetic lineations are subhorizontal and are also subparallel to the pluton elongation. However in the centre of the pluton, the foliations are WNW–ESE striking and are parallel to the magnetic lineation trends (Sant’Ovaia et al., 2000). In the Águas Frias-Chaves pluton magnetic foliations are parallel to the borders of the pluton with E–W strikes and with outward dips (ca 30°). Magnetic lineations are

WNW–ESE trending and with shallow plunges (Fig. 2). Both, magnetic lineations and foliations are concordant for all the pluton. It must be noted that ASM lineations and foliations are similar in central area of the Vila Pouca de Aguiar pluton and the Águas Frias-Chaves pluton.

#### 4.1.2. Gravimetry

The isovalue contour line gradients of the Bouguer anomaly map (Fig. 3) for the Vila Pouca de Aguiar pluton clearly indicates that the pluton is bounded by overall inward dipping contact surfaces. A region of pronounced minima is present at the northern end of the pluton, toward a still more pronounced one corresponding to the Águas Frias-Chaves pluton. The Bouguer anomaly map shows that the Águas Frias-Chaves pluton appears as a depression with anomalies ranging from −55 to −61 mGal. The pluton is well outlined by the −55 mGal contour line with a gradient inward to the pluton. A region of pronounced minima (<63 mGal) is present at the southwestern border of the pluton, which corresponds to the alluvium deposits from Chaves graben (Fig. 3a).

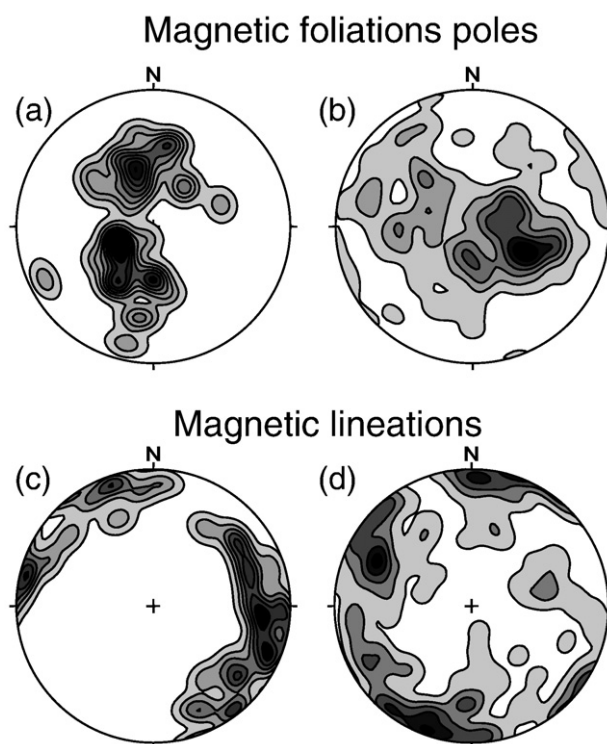


**Fig. 2.** Orientation diagram of magnetic foliations poles and lineations: (a) and (c) from the Águas Frias-Chaves pluton; (b) and (d) from the Vila Pouca de Aguiar pluton. Projection in Schmidt net, lower hemisphere (1, 2, 3, 4, 5, 6, 7 e 8° contours).

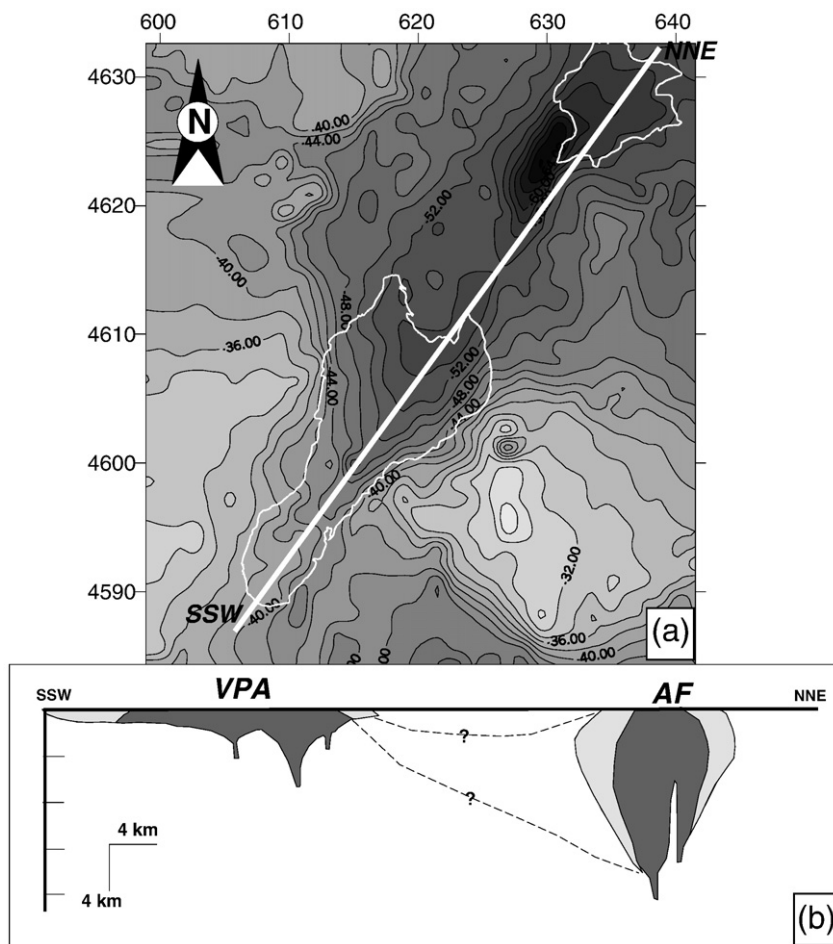


Fig. 3. (a) Bouguer gravity anomaly map of the Vila Pouca de Aguiar and the Águas Frias-Chaves plutons and surrounding areas (in mGal). (Sketch map of the plutons in white); (b) Cross-section parallel to the PRVF of the Vila Pouca de Aguiar and Águas Frias-Chaves plutons obtained after gravimetric data inversion and AMS data.

In the Vila Pouca de Aguiar pluton the residual anomaly map yields a negative signature for the pluton of about  $-4$  to  $-8$  mGal in amplitude, and a positive anomaly at the east and west of the area, correlates with the metasediments. The residual anomaly map for the Águas Frias-Chaves pluton yields a negative signature for the studied pluton of about  $0$  to  $-6$  mGal in amplitude, and a positive anomaly at the east and west of the area, that can be correlated with metasediments. The residual anomaly map satisfactorily isolates the effect of the studied pluton, except at its southwestern part, where the zero contour level doesn't close. In this sector there is a separation between the zero contour level, elongated parallel to a graben (related to PRVF) and with a NNE-SSW trending outward the studied area limits. The negative anomaly of the Águas Frias-Chaves pluton is related to a lower density of the granite than that of the surrounding country-rocks. In the graben, we have also a strong negative residual anomaly ( $-12$  mGal) due to the lower density of the alluvium deposits.

Gravity modelling of each one of the plutons pointed out that their shapes are quite different (Sant'Ovaia et al., 2000; Sant'Ovaia and Noronha, 2005b) (Fig. 3b). For the Vila Pouca de Aguiar pluton the gravity modelling discloses that the pluton is laccolithic and does not exceed 1 km in thickness over more than 60% of its outcrop area. Within a triangular area facing the northern end of the pluton, and extending somewhat to the north under the northern cover rocks, the pluton's floor becomes deeper than 1 km under the present surface. The skeleton lines joining the deepest zones form a N-trending valley at the western side of this triangular area, and a NE-trending one at its eastern side. To the south, these two valleys merge into a single one extending south within the PSG type. Along the western valley, three

narrow areas, circular in map view and up to 5 km deep, could be viewed as root-zones for this pluton. The southern one is located right in the center of the inner and least susceptible domain of the PSG. Gravity modelling of the Águas Frias-Chaves pluton suggests that its floor presents depth values which reach 12 km. In the central zone,

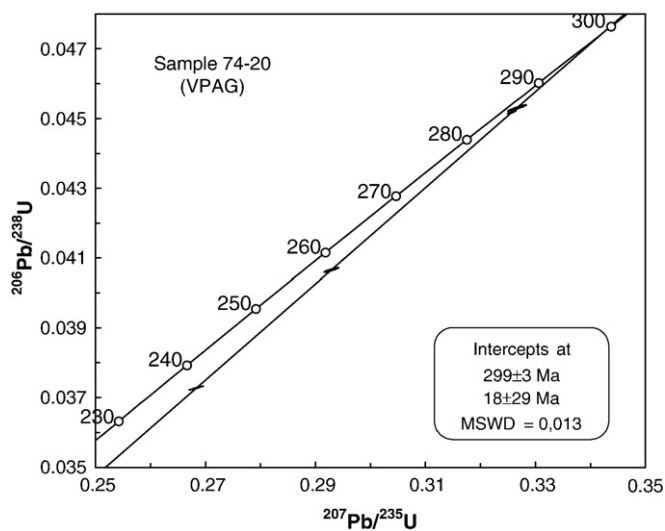


Fig. 4. U-Pb Concordia diagram showing analytical data for zircons fractions from one sample (74-20) of the Vila Pouca de Aguiar granite, northern Portugal.

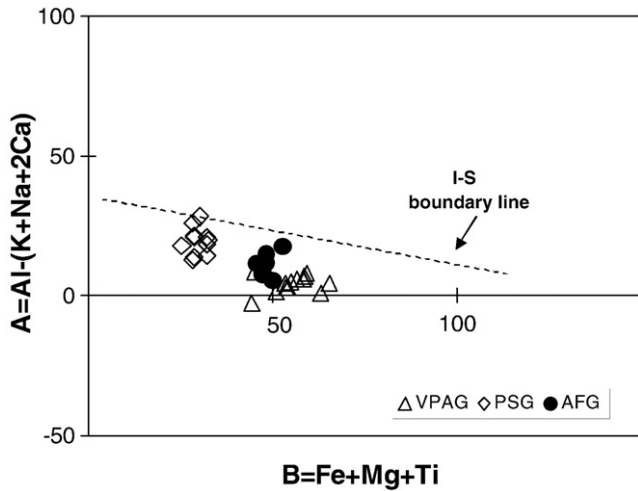


Fig. 5. A versus B parameters, in millications, (Debon and Le Fort, 1983) from the Vila Pouca de Aguiar, Pedras Salgadas and Águas Frias granites, northern Portugal; I-S boundary line from Villaseca et al. (1998a).

under the outcrop of the two-mica granite, there is the main volume of the pluton, with floor depths reaching 16 km. In this zone it is located a deep conduit which can be assumed as a feeding root. At the

south limit, the pluton floor seems to extent in SSW direction under the cover rocks with shallow depth values.

The VPAG can be considered as a sill while the PSG 2–3 km thick over 2/3 of its outcrop area, is thicker and forms the main volume of the Vila Pouca de Aguiar pluton. The Águas Frias-Chaves pluton has a greater thickness ( $\approx 10$  km) and belongs to the wedge-floored pluton type of Ameglio et al. (1997). Nevertheless, these data didn't underline any differences in shape of the two granites from the Águas Frias-Chaves pluton. Gravity data also suggest that the Águas Frias-Chaves pluton is more rooted than the Vila Pouca de Aguiar pluton and show that there is a connection of the two gravimetric anomalies in depth.

#### 4.2. Geochemistry

##### 4.2.1. U–Pb geochronology

The U–Pb zircon data were carried out on four zircon fractions of one sample (74–20) from the VPAG. A typological study (Pupin, 1980) has allowed the identification of several zircon types (Martins and Noronha, 2000). The zircons are very limpid, colourless or light yellow colour. The BSEM images of the long prismatic zircons revealed an inner zone surrounded by a complex magmatic zoning. Some of them have cores that could correspond to an earlier magmatic crystallization. The prismatic acicular and flat zircons are more homogeneous crystals devoid of cores and showing generally a faint zoning with dominantly oscillatory internal structures. The four zircon

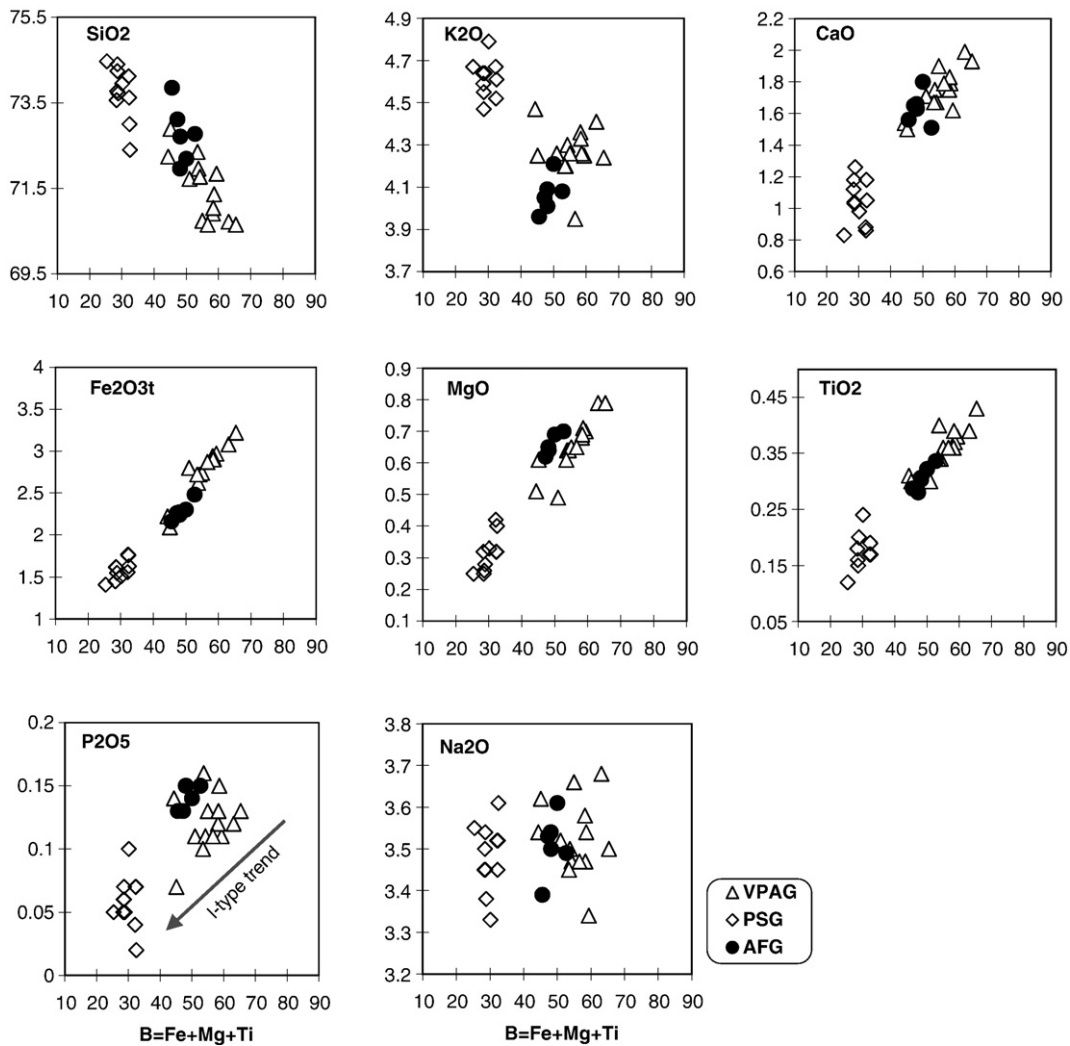


Fig. 6. Variation diagrams of selected major (wt.%) elements vs. parameter B = Fe + Mg + Ti (in millications) from the Vila Pouca de Aguiar, Pedras Salgadas and Águas Frias granites, northern Portugal.

fractions are concordant and define a line (MSWD of concordance = 0.013, probability of fit = 0.99) intersecting the Concordia at  $299 \pm 3$  Ma (Fig. 4). This upper intercept at 299 Ma is interpreted as the crystallization age of the biotite granite.

#### 4.2.2. Major, trace and rare earth elements

The studied granites are K-rich monzogranites ( $K_2O/Na_2O = 1.1$ – $1.4$  and  $K_2O + Na_2O = 7.4$ – $8.5$ ) and have a weakly peraluminous character with the molecular ratio  $Al_2O_3/(CaO + Na_2O + K_2O)$  between 0.99 and 1.07. The low normative corundum values ( $<0.7\%$  in VPAG + AFG and close to 1% in PSG) are consistent with their being I-type (Chappell and White 1992; Villaseca et al., 1998a) as seen in the A–B diagram (Fig. 5). The VPAG and the AFG share comparable chemistry but different from that of the PSG. This granite is enriched in  $SiO_2$  and  $K_2O$  and contains the lowest CaO,  $Fe_2O_3$ , MgO,  $TiO_2$ ,  $P_2O_5$ , Sr and Zr contents (Table 2).

The variation diagrams were plotted against parameter  $B = Fe + Mg + Ti$  (in millications) used as the differentiation index (Debon and Le Fort, 1983) because it shows a better discrimination than does  $SiO_2$ . In VPAG + AFG it was possible to identify two different trends: an incompatible behaviour for  $SiO_2$  and a compatible behaviour for  $K_2O$ ,  $Fe_2O_3$ ,  $TiO_2$ , MgO, CaO,  $P_2O_5$ , Ba and Zr (Figs. 6 and 7). The samples of the PSG, for most of the elements, show small variations, although significant, defining a discordant evolutionary trend relative to the other two granites (e.g.  $K_2O$ , CaO, Ba and Y plots). However the variations of most of the elements are not correlated with the simultaneous decrease of Fe, Mg and Ti and therefore with the differentiation index, suggesting that the major and some trace element variations can be related to the proportion of felsic minerals (potassic feldspar and/or plagioclase) in this granite. In the variation diagrams (Figs. 6 and 7) the presence of two distinct geochemical and genetic units, VPAG + AFG and PSG is suggested: (1) a small compositional gap between VPAG + AFG and PSG appears and (2) a change in slope trend, namely of Sr, Y and Rb contents. The observed variations trends in the peripheral granites of the two plutons (AFG + VPAG) as well as the plot of the samples throughout the same evolution line suggest that these two granites had similar genesis.

The three granites have similar REE concentrations (Table 2) and normalized patterns, (Fig. 8). All the granites have low  $\Sigma REE$  and wing-shaped patterns with  $(La/Yb)_N$  ranging from 3.25 to 9.29 for the VPAG, 5.12 to 6.39 for the AFG and 2.90 to 6.02 for PSG. They show a pronounced negative Eu anomaly ( $Eu/Eu^*$ ) ranging from 0.35–0.50 in the VPAG through 0.30–0.35 for the AFG to 0.29–0.36 in the PSG. The larger negative Eu anomaly corresponds to the samples richer in  $SiO_2$  and more depleted in Sr (PSG) indicating that feldspar fractionation was a common process during the evolution of this granitic magma.

The major and trace element trends in the studied granites are similar to those observed by Chappell and White (1992) in fractionated I-type granites from SE Australia that is, an increase in Th, Y and HREE contents. The decrease in  $P_2O_5$  shown in studied granites is also an important criterion for distinguishing I-type granites because apatite reaches saturation in metaluminous and weakly peraluminous magmas (Chappell and White, 1992). The same geochemical trends were observed for I-type granites in other regions of the Iberian Peninsula, namely in the Spanish Central System (Villaseca et al., 1998b).

#### 4.2.3. Isotopic data

Five samples of the VPAG define a good whole-rock Rb–Sr isochron, which yields an age of  $298 \pm 9$  Ma (Fig. 9) and an initial  $^{87}Sr/^{86}Sr$  ratio of  $0.70710 \pm 0.00084$  (MSWD = 1.4; probability of fit = 0.24). This age is in full agreement with the U–Pb zircon age of  $299 \pm 3$  Ma obtained for the same granite. The plot of the PSG samples also define a good whole-rock Rb–Sr isochron yielding an age of  $297 \pm 14$  Ma (Fig. 9) and an initial  $^{87}Sr/^{86}Sr$  isotopic ratio of  $0.7052 \pm 0.0022$  (MSWD = 2.3; probability of fit = 0.075). The AFG samples (three samples) present a so small dispersion that it was not possible to obtain a whole-rock Rb–Sr isochron. However the field relations, late-tectonic emplacement along the same tectonic lineation, led us to suppose that they have similar intrusion ages. The available U–Pb and Rb–Sr ages clearly indicate a post- $D_3$  emplacement for these granites which agree with the geological data and the AMS studies (Sant'Ovaia, 2000; Sant'Ovaia et al., 2000), as well as to the geochronologic data available for post- $D_3$  Variscan granitoids in Northern Portugal (Pinto et al., 1987; Dias et al., 1998; Martins et al., 2001; Mendes and Dias, 2004).

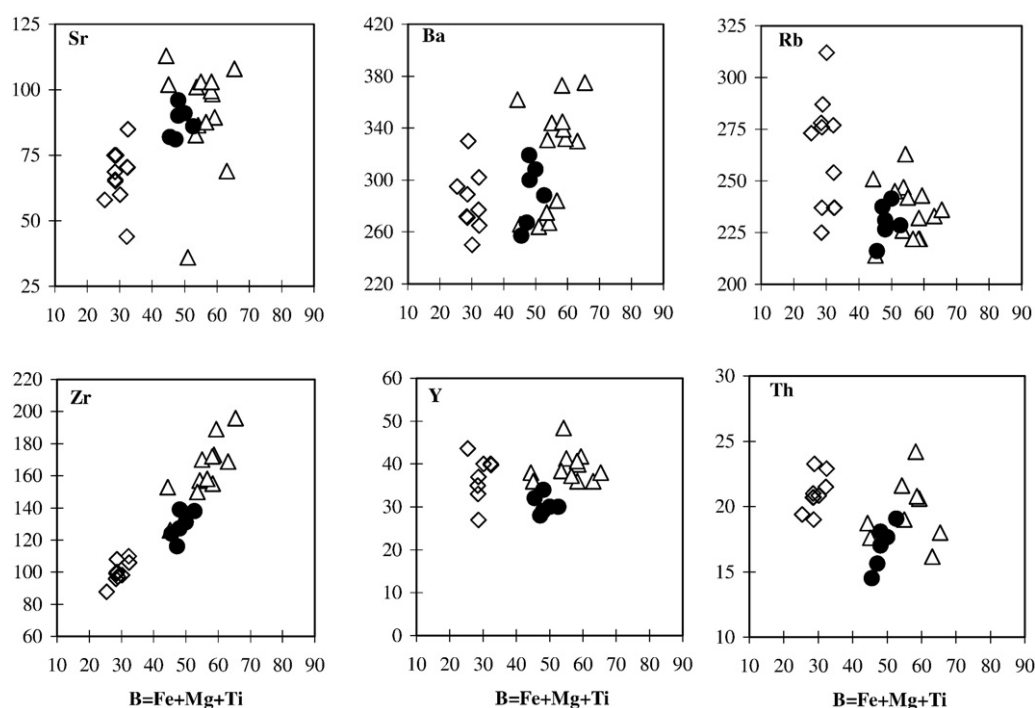


Fig. 7. Variation diagrams of selected trace (ppm) elements vs. parameter  $B = Fe + Mg + Ti$  (in millications) from the Vila Pouca de Aguiar, Pedras Salgadas and Águas Frias granites, northern Portugal. Symbols as in Fig. 6.

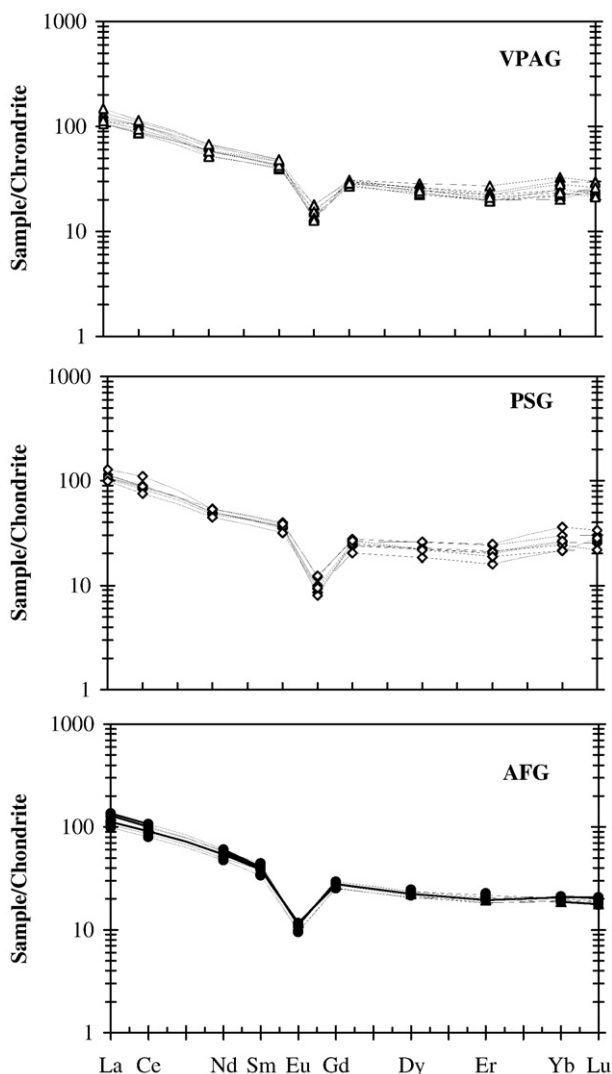


Fig. 8. Chondrite-normalized REE distribution from the Vila Pouca de Aguiar, Pedras Salgadas and Águas Frias granites, northern Portugal. Normalization values from Evensen et al. (1978).

In terms of Sr and Nd compositions, the VPAG and the AFG present the same rather little evolved isotope composition with  $(^{87}\text{Sr}/^{86}\text{Sr})_{299}$  between 0.7067 to 0.7071 and 0.7076 to 0.7079, respectively, whereas  $\epsilon\text{Nd}_{299}$  is very similar in both granites around to  $-2.5$  (Table 2). The PSG yields the less evolved isotopic composition with  $(^{87}\text{Sr}/^{86}\text{Sr})_{299}$  between 0.7044 and 0.7050 and  $\epsilon\text{Nd}_{299} = -2.0$ . These granites are significantly less radiogenic in Sr but more radiogenic in Nd than most of the Variscan granitoid rocks of Iberian Peninsula as well as most of the European Variscan granites (Cuesta, 1991; Schaltegger and Corfu, 1992; Cocherie et al., 1994; Forster et al., 1999; Paquette et al., 2003 and references therein). However, we must note that the post- $D_3$  granites from Northern Portugal, all have a weakly evolved isotopic composition (Silva and Neiva, 2004; Mendes and Dias, 2004).

Whole-rock oxygen isotope ( $\delta^{18}\text{O}$  VSMOW) values for seven representative samples of the studied granites, range from  $+9.7\%$  to  $+11.0\%$ . These data suggest that the Vila Pouca de Aguiar, the Pedras Salgadas and the Águas Frias granites were produced by partial melting of meta-igneous crustal source, I-type granites, (Dallai et al., 2002; Hoefs, 2004).

### 5. Discussion

The modelling of the residual gravity indicates that the shapes of the two granite plutons are quite different: the Vila Pouca de Aguiar

pluton is laccolithic in overall shape and the Águas Frias-Chaves pluton has a greater thickness ( $\approx 10$  km) and is a thicker and deeply rooted body (Fig. 3b). However gravity data show a connection of the two gravimetric anomalies which point out that the magma batches upwelled from the PRVF. In the Vila Pouca de Aguiar pluton we can consider a first magma upwelling for the VPAG developing a sill by a dominantly southward magma flow as is attested by the NNE–SSW magnetic lineations. Then, the more voluminous PSG batch upwelled with upward ballooning and dominant WNW–ESE dilation perpendicular to the fault zone as shown by the magnetic lineations. The latter intrusion took place, however, in a yet non-consolidated VPAG, as attested by the overall concordant magnetic foliations. The Águas Frias-Chaves pluton gravity and ASM data indicate that two granite types ascended and emplaced in a continuous event forming a thick pluton that was fed through a deeper root within PRVF. The magma upwelling involved also a WNW–ESE dilation similar to the PSG ascending mechanism.

We assume that the differences in geometry of the two plutons are related to the depth of PRVF in the sector of Águas Frias-Chaves. This fault is also a preferential location for several  $\text{CO}_2$  rich thermal water springs, that reach temperatures of  $74^\circ\text{C}$  near the Águas Frias-Chaves pluton, at Chaves, while in the Vila Pouca de Aguiar pluton temperature is much lower,  $15^\circ\text{C}$  at Pedras Salgadas. Several authors have suggested a deep-seated (mantle) origin for most of the  $\text{CO}_2$  in these mineral waters (Aires-Barros et al., 1998; Marques et al., 2000). We think that the hotter water from Chaves spring can be explained by a great depth of the aqueous layer for this sector of PRVF which is

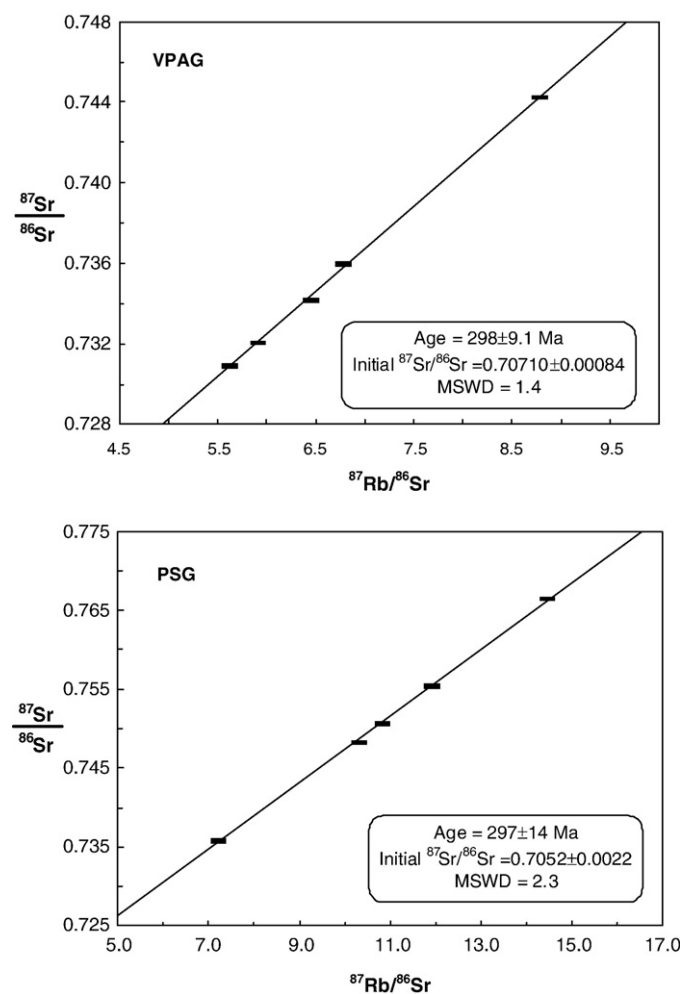


Fig. 9. Rb–Sr whole-rock isochrons from the Vila Pouca de Aguiar granite (VPAG) and the Pedras Salgadas granite (PSG). Age errors are quoted at the 95% confidence level.

consistent with a deeper root and thickness for the Águas Frias-Chaves pluton than for the Vila Pouca de Aguiar pluton.

The U–Pb zircon age ( $299 \pm 3$  Ma) can be considered the emplacement age of the Vila Pouca de Aguiar pluton. The late-tectonic emplacement along the same tectonic lineation, led us to suppose that the Águas-Frias-Chaves pluton has a similar intrusion age. This age allows the precise dating of the end of late Variscan  $D_3$  tectonic phase (ca 300 Ma) which fits with that obtained by Dias et al. (1998) and Aguado et al. (2005). The agreement between the Rb–Sr ( $298 \pm 9$  Ma and  $297 \pm 14$  Ma) and U–Pb ( $299 \pm 3$  Ma) ages suggests that the granitic magmas had an isotopically homogeneous source. The rather low initial ratios  $^{87}\text{Sr}/^{86}\text{Sr}$  values (0.7044–0.7079) indicate that lower crustal material had been involved in the partial melting (Faure, 1986; Chappell, 1999; Hoefs, 2004). The initial Nd isotopic ratios (–2.0 to –2.5) are also compatible with a significant contribution of deep crustal sources in the genesis of these granites. According to some authors (Forster et al., 1999; Villaseca et al., 1999) the thermal productivity of the lower crust is high enough to promote extensive melting and thus granite generation during the Variscan orogeny. However additional heat from mantle-derived underplated material cannot be ruled out, but does not seem to be required to explain the granites.

The Rb–Sr isotopic compositions, as well as the weakly peraluminous signature of these granites are consistent with I-type affinity. Magmas related to I-type magmatism can evolve progressively by fractional crystallization and the rocks tend towards saturation in Al. Other I-type magmas, formed directly by partial melting, are generally more oversaturated in Al as are the corresponding S-type melts derived from more peraluminous source rocks (Chappell, 1999). Although the fractionation of the studied granites is not strong, the distinctive features of such fractionation that they show, are clear. The high Rb and particularly the very low Sr contents, clearly indicate that there has been fractionation of feldspars from a felsic melt. Moreover, these granites show high HREE, Th and Y (and low P) contents which is a common evolutionary trend in I-type granite suites.

The existence of a positive correlation between the differentiation index and Zr (Fig. 7) and an inverse correlation between that index and Yb (not shown) imply an inverse correlation Zr–Yb, which means that during the fractional crystallization Zr decreases while Yb increases. The increase in Yb cannot be explained only by zircon fractionation, since this mineral has a high  $K_D$  for Yb. Thus it is necessary to admit that the role played by the zircon is counterbalanced by major mineral fractionation and by the restricted crystallization of other REE-rich minerals (Chappell, 1999). In this way, the lower content of P (phosphorus) in I-type granitic magmas (Watson and Harrison, 1984; Bea et al., 1992) reduces the amount of REE-rich phosphates (apatite, monazite) or makes impossible their crystallization (e.g. xenotime). This contrasted behaviour with respect to the more peraluminous (and P-rich) S-type granites contributes to the lack of HREE (and Y) depletion (see also Villaseca et al., 1998b). Increasing contents of HREE in felsic granites is apparently a consequence of the very low P contents in I-type granitic melts, in which accessory P-rich minerals that contain HREE do not precipitate (e.g. xenotime), thus those elements increase in the residual melt (Chappell, 1999). The behaviour of phosphorus can be explained in terms of the strong control of the melt peraluminosity on apatite solubility (Chappell and White, 1992; Pichavant et al., 1992). The depletion in P during differentiation of these biotite granites is due to two causes: i) the low P content in parental I-type granitic melts due to the low apatite solubility and ii) the progressive apatite (and monazite, in lesser amounts) crystallization. Because apatite is much more soluble in peraluminous melts, P is more abundant in the S-type melts and some S-type granites as fractionate, give rise to a per-phosphorous enrichment trend (Bea et al., 1992). This leads to contrasts in the abundance of P and of elements such Y, the REE and Th, between strongly fractionated I- and S-type granites (Chappell, 1999).

The protolith nature of post- $D_3$  Variscan differentiated I-type granites is a matter of debate, the lack of appropriated sources in the vicinity of the Variscan plutons suggests that granite sources in orogenic areas are not the outcropping metamorphic rocks but are located in deeper crustal levels. Villaseca et al. (1998b, 1999) and Villaseca and Herreros (2000) assumed an almost purely crustal origin for the Spanish Central System (SCS) granitoids mainly from meta-igneous sources. The most suitable crustal source rocks are felsic granulites that represent the 95% of the total volume of xenoliths from the Variscan lower crust of the SCS. The isotopic compositions of the studied granites, namely the VPAG and the AFG, match the  $^{87}\text{Sr}/^{86}\text{Sr}_i$  and  $\epsilon\text{Nd}$  values of the felsic xenoliths suggesting that this kind of rock could be a potential source (Fig. 10). Although the Nd isotopic data from PSG fit that of the granulites xenoliths, this granite displays a less radiogenic Sr composition. Furthermore models from crustal data show that there are no significant lateral inhomogeneities in crustal structure in contrast to the heterogeneous Variscan surface geology (Wedepohl, 1995).

On the other hand the  $\delta^{18}\text{O}$  values of these granites (in the range of 9.7‰ to 11.0‰) also support a meta-igneous source. In fact it is well known that granulites constitute the dominant rock type in the lower crust (Wedepohl, 1995; Hoefs, 2004) and similar oxygen isotopes results have been obtained from lower crustal granulite xenoliths which exhibit a large range in  $\delta^{18}\text{O}$  values from 5.4 to 13.5‰. Felsic meta-igneous granulites are significantly enriched in  $\delta^{18}\text{O}$  with an average  $\delta^{18}\text{O}$  values around 10‰ (Hoefs, 2004) which are similar to those obtained for the studied granites. Provided that the VPAG, the PSG and the AFG had not been affected by subsolidus isotope exchange, its isotopic composition could reflect the isotopic composition of the source, among other factors.

A model of a mantle–crust interaction could be supported by the Sr–Nd isotopic signatures and the presence of some tonalitic and granodioritic microgranular enclaves within these granites. The frequent presence of basic to intermediate igneous enclaves in granitic rocks, is considered usually as an evidence for hybridization with a mantle-derived component (Vernon, 1984; Didier, 1987; Orsini et al., 1991; Barbarin and Didier, 1992; Dias and Leterrier, 1994; Moreno-Ventas et al., 1995; Bea et al., 1999; Collins et al., 2000; Dias et al., 2002; Bonin, 2004; Janousek et al., 2004; Silva and Neiva, 2004; Renna et al., 2006; Slaby and Martin, 2008). However a simple mixing model (not shown) with a basic pole with a Sr–Nd isotopic composition close to bulk-earth values (as used by Moreno-Ventas et al., 1995) and an acid end-member corresponding to the average of lower crustal xenoliths (Villaseca et al., 1998b) suggest an enormous

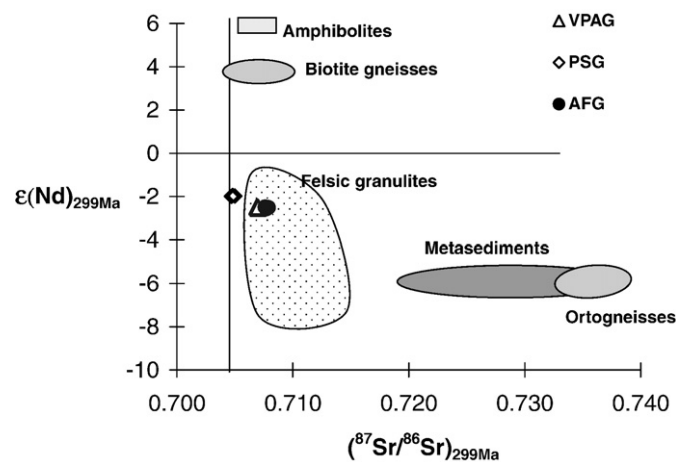


Fig. 10. Initial  $^{87}\text{Sr}/^{86}\text{Sr}$  vs. initial  $\epsilon\text{Nd}$  plot of the Vila Pouca de Aguiar, Pedras Salgadas and Águas Frias granites, northern Portugal, compared with compositional fields from potential sources in the Variscan basement. Data sources: metasediments (Beetsma, 1995); ortogneisses, biotite gneisses and amphibolites (Noronha and Leterrier, 2000); felsic granulites (Villaseca et al., 1999). All isotopic ratios are calculated to a common age of 299 Ma.

contribution of more than 50% of the mantle-derived component, making this process unrealistic taking into account the scarcity of basic rocks and mafic enclaves in the studied sector. Nevertheless, the relative uniformity in the  $\varepsilon_{\text{Nd}}^{\text{DT}}$  values for the three granites ( $\varepsilon_{\text{Nd}}^{\text{DT}} = -2.5$  in the VPAG + AFG and  $-2.0$  in the PSG) led us to consider the existence of an isotopically moderately heterogeneous lower crustal source to be more consistent than mixing of mantle-derived and crustal melts from very contrasted compositional sources, from lower- and upper-crustal levels.

Gravimetry, AMS and geochemical data together with Sr–Nd isotopic results suggest that the Vila Pouca de Aguiar pluton (VPAG + PSG) grew as two granitic magma batches which accumulate in the same emplacement level but, without efficient mixing, prevent a more isotopic homogenised pluton. However the Águas Frias granite (AFG) and the Vila Pouca de Aguiar granite (VPAG) grew as a result of the emplacement of similar granite magma batches.

## 6. Conclusions

The Vila Pouca de Aguiar and Águas Frias–Chaves plutons are an example of post- $D_3$  differentiated Variscan I-type granites in northern Portugal (NW Iberian Peninsula). Both plutons, outcropping separately ca 20 km one from the other, are made up mainly of K-rich monzogranites that have a very weak peraluminous character. These granites share similar geochemical features (major, trace and rare earth elements) and have an I-type subalkaline affinity. The available data suggest that the VPAG and the AFG are related to similar initial magma batches, but different from the PSG, which are supported by their isotopic compositions and also by gravimetry and AMS results.

The U–Pb zircon analyses yield a consistent age of  $299 \pm 3$  Ma which is considered to be the emplacement age of the Vila Pouca de Aguiar pluton and probably reflects also the intrusion age of the cogenetic Águas Frias–Chaves pluton. This age is in agreement with the post- $D_3$  character of these granites and constrains the timing of the last ductile Variscan deformation phase. The emplacement of granite magmas is coeval with late Variscan strike slip fault in an extensional tectonic regime, large scale uplift and crustal thinning.

The integration of different data suggests that both plutons have the same feeding zone aligned within the Penacova–Régua–Verin fault and have the same structure which is related to late Variscan phases. Nevertheless the pluton shapes are quite different, the Vila Pouca de Aguiar pluton is laccolithic in overall shape whereas the Águas Frias–Chaves pluton has a greater thickness and is a deeply rooted body. These differences are consistent with a great depth for the Penacova–Régua–Verin strike slip fault in the northernmost outcrop's location of the Águas Frias pluton.

The available geological, geochemical and isotopic data led us to propose a model of partial melting of a meta-igneous lower continental crust rather than an open-system mantle–crust interaction. The interaction between the continental crust and invading mafic magmas could have been limited to mere heat transfer and, perhaps, local intermingling.

## Acknowledgements

This research was carried out at the Geology Center (Porto University), an R and D unit from Portuguese Foundation of Science and Technology. We acknowledge Prof. J. Touret and Prof. Carlos Villaseca for their helpful comments which greatly improved the original manuscript. The authors wish to thank J. Letierrier for his assistance at GRPG (Nancy-France) and for the fruitful discussions. Prof. Gil Ibarguchi (País Vasco University, Spain) and Prof. Clemente Recio (Salamanca University, Spain) are thanked for their diligence in the performance of Sr–Nd and oxygen isotope analyses. Available regional gravity data were kindly supplied by Professor L. Mendes Victor (Portuguese Institute of Space and Earth Sciences).

## Appendix A. Geographical coordinates: UTM kilometric system of geochemical sampling, from the granites of the Vila Pouca de Aguiar and the Águas Frias–Chaves plutons

Samples	Granites	UTM	
74-3	VPAG	607.38	4592.88
74-12	VPAG	609.30	4596.45
74-15	VPAG	611.67	4594.18
74-16	VPAG	607.91	4595.31
74-9	VPAG	611.74	4597.38
74-5	VPAG	617.02	4599.28
74-20	VPAG	609.83	4591.96
74-4B	VPAG	610.93	4592.80
46-2	VPAG	616.82	4612.55
61-13	VPAG	625.92	4606.47
61-6A	VPAG	622.56	4610.39
61-6B	VPAG	624.56	4607.18
60-14	VPAG	614.35	4609.67
60-15	VPAG	614.50	4608.51
60-16	VPAG	615.11	4606.44
60-11	VPAG	620.06	4610.43
60-12	VPAG	618.79	4611.48
60-17	PSG	615.41	4603.82
60-13	PSG	616.73	4609.46
60-10	PSG	617.49	4605.96
60-18	PSG	615.89	4604.17
60-19	PSG	616.06	4602.63
61-6	PSG	621.69	4608.15
74-8	PSG	615.25	4600.26
74-7	PSG	614.91	4599.56
74-11	PSG	615.98	4601.09
60-1	PSG	614.98	4602.56
60-2	PSG	614.84	4603.42
CV1	AFG	632.25	4624.36
CV2	AFG	638.82	4627.00
34-4	AFG	635.65	4631.03
CV-8	AFG	637.75	4630.81
CV-11	AFG	634.98	4630.51
CV-13	AFG	637.50	4628.92

## References

- Aguado, B.V., Azevedo, M.R., Schaltegger, U., Martínez Catalán, J.R., Nolan, J., 2005. U–Pb zircon and monazite geochronology of Variscan magmatism related to syn-convergence extension in Central Northern Portugal. *Lithos* 82, 169–184.
- Aires-Barros, L., Marques, J.M., Graça, R.C., Matias, M.J., Weijden, C.H., Kreulen, R., Eggenkamp, H.G.M., 1998. Hot and cold  $\text{CO}_2$ -rich mineral waters in Chaves geothermal area (northern Portugal). *Geothermics* 27, 89–107.
- Almeida, A., Martins, H.C.B., Noronha, F., 2002. Hercynian acid magmatism and related mineralisations in Northern Portugal. *Gondwana Research* 5 (2), 423–434.
- Ameglio, L., Vignerresse, J.L., Bouchez, J.L., 1997. Granite pluton geometry and emplacement mode inferred from combined fabric and gravity data. In: Bouchez, J.L., Hutton, D.H.W., Stephens, W.E. (Eds.), *Granite: From Segregation of Melt to Emplacement Fabrics*. Kluwer Academic Publishers, Dordrecht.
- Arthaud, F., Matte, Ph., 1975. Les décrochements tardi-hercyniens du Sud-Ouest de l'Europe. *Géométrie et essai de reconstitution des conditions de la déformation*. *Tectonophysics* 25 (1/2), 139–171.
- Barbarin, B., Didier, J., 1992. Genesis and evolution of mafic microgranular enclaves through various types of interaction between coexisting felsic and mafic magmas. *Transactions of Royal Society of Edinburgh Earth Science* 83, 145–153.
- Bea, F., Fershtater, G.B., Corretgé, L.G., 1992. The geochemistry of phosphorus in granite rocks and the effects of aluminium. *Lithos* 29, 43–56.
- Bea, F., Montero, P., Molina, J.F., 1999. Mafic precursors, peraluminous granitoids, and late lamprophyres in the Avila batholith: a model for the generation of Variscan batholiths in Iberia. *Journal of Geology* 107 (4), 399–419.
- Beetsma, J.J., 1995. The late Proterozoic/Paleozoic and Hercynian crustal evolution of the Iberian Massif, Northern Portugal. Ph.D. Thesis. Vrije Universiteit Amsterdam.
- Bonin, B., 2004. Do coeval mafic and felsic magmas in post-collisional to within-plate regimes necessarily imply two contrasting, mantle and crustal, sources? A review. *Lithos* 78, 1–24.
- Bouchez, J.L., 1997. Granite is never isotropic: an introduction to AMS studies of granitic rocks. In: Bouchez, J.L., Hutton, D.H.W., Stephens, W.E. (Eds.), *Granite: From Segregation of Melt to Emplacement Fabrics*. Kluwer Academic Publishers, Dordrecht.
- Bouchez, J.L., Bernier, S., Rochette, P., Guineberteau, B., 1987. Log des susceptibilités magnétiques et anisotropies de susceptibilité dans le granite de Beauvoir: conséquences pour sa mise en place. *Géologie de la France, BRGM* 2 (3), 223–232.
- Brink, A.H., 1960. Petrology and ore geology of the Vila Real–Sabrosa–Vila Pouca de Aguiar region, Northern Portugal. *Comunicações dos Serviços Geológicos de Portugal* 43, 1–143.

- Cabral, J., 1995. Neotectónica em Portugal Continental. PhD Thesis, Memória 31, Instituto Geológico Mineiro, Lisboa.
- Chappell, B.W., 1999. Aluminium saturation in I- and S-type granites and the characterization of fractionated haplogranites. *Lithos* 46, 535–551.
- Chappell, B.W., White, A.J.R., 1992. I- and S-type granites in the Lachlan Fold Belt. *Transactions of the Royal Society of Edinburgh Earth Science* 83, 1–26.
- Cocherie, A., Rossi, Ph., Fouillac, A.M., Vidal, Ph., 1994. Crust and mantle contributions to granite genesis – an example from the Variscan batholith of Corsica, France, studied by trace-element and Nd–Sr–O-isotope systematics. *Chemical Geology* 115, 173–211.
- Collins, W.J., Richards, S.R., Healy, B.E., Ellison, P.I., 2000. Origin of heterogeneous mafic enclaves by two-stage hybridisation in magma conduits (dykes) below and in granitic magma chambers. *Transactions of the Royal Society of Edinburgh Earth Science* 91, 27–45.
- Cordell, L., Henderson, R.G., 1968. Iterative three dimensional solution of gravity anomaly using a digital computer. *Geophysics* 33, 596–601.
- Cuesta, A., 1991. *Petrología Granítica Del Plutón De Caldas De Reyes (Pontevedra, España)*. Estructura, Mineralogía, Geoquímica Y Petrogenesis. Univ. Oviedo. O. Castro Ph.D. Thesis. Laboratorio Xeolóxico de Laxe, Série Nova Terra 5, 1–363.
- Dallai, L., Ghezzi, C., Turi, B., Vesica, P.L., 2002. Oxygen isotope geochemistry of the Granite Harbour Intrusives, Wilson Terrane, Northern Victoria Land, Antarctica. *Mineralogy and Petrology* 75, 223–241.
- Debon, F., Le Fort, P., 1983. A chemical–mineralogical classification of common plutonic rocks and associations. *Transactions of the Royal Society of Edinburgh Earth Science* 73, 135–149.
- Dias, G., Leterrier, J., 1994. The genesis of felsic–mafic plutonic associations: a Sr and Nd isotopic study of the Hercynian Braga Granitoid Massif (Northern Portugal). *Lithos* 32, 207–223.
- Dias, R., Ribeiro, A., 1995. The Ibero-Armorican Arc: a collision effect against an irregular continent? *Tectonophysics* 246, 113–128.
- Dias, G., Leterrier, J., Mendes, A., Simões, P.P., Bertrand, J.M., 1998. U–Pb zircon and monazite geochronology of post-collisional Hercynian granitoids from the Central Iberian Zone (Northern Portugal). *Lithos* 45, 349–369.
- Dias, G., Simões, P.P., Ferreira, N., Leterrier, J., 2002. Mantle and crustal sources in the genesis of late-Hercynian granitoids (NW Portugal): geochemical and Sr–Nd isotopic constraints. *Gondwana Research* 5 (2), 287–305.
- Didier, J., 1987. Contribution of enclave studies to the understanding of origin and evolution of granitic magmas. *Geologische Rundschau* 76, 41–50.
- Evensen, N.M., Hamilton, P.J., O’Nion, R.K., 1978. Rare-earth abundances in chondritic meteorites. *Geochemical and Cosmochimica Acta* 42, 1199–1212.
- Farias, P., Gallastegui, G., Gonzalez Lodeiro, F., Marquinez, J., Martin Parra, L.M., Martinez Catalan, J.R., Pablo Maciá, J.G., Rodriguez Fernandez, L.R., 1987. Aportaciones al conocimiento de la litostratigrafía y estructura de Galicia Central. In: IX Reunión de Geología do Oeste Peninsular, Porto. Memórias do Museu e Laboratório Mineralógico e Geológico da Faculdade de Ciências da Universidade do Porto 1, 411–431.
- Faure, C., 1986. *Principles of isotope geology*. John Wiley & Sons, New York.
- Ferreira, N., Iglésias, M., Noronha, F., Pereira, E., Ribeiro, A., Ribeiro, M.L., 1987. Granitoides da Zona Centro Ibérica e seu enquadramento geodinâmico. In: Bea, F., Carnicero, A., Gonzalo, J., Lopez Plaza, M., Rodriguez Alonso, M. (Eds.), *Geología de los Granitoides y Rocas Asociadas del Macizo Hesperico*. Editorial Rueda, Madrid, pp. 37–51. Libro de Homenaje a L.C. García de Figurella.
- Forster, H.J., Tischendorf, G., Trumbull, R.B., Gottsmann, B., 1999. Late collisional granites in the Variscan Erzgebirge, Germany. *Journal of Petrology* 40 (11), 1613–1645.
- Govindaraju, K., Mevelle, G., 1987. Fully automated dissolution and separation methods for inductively coupled plasma atomic emission spectrometry rock analysis. Application to the determination of rare earth elements. *Journal of Analytical Atomic Spectrometry* 2, 615–621.
- Hoefs, 2004. *Stable Isotopic Geochemistry*, 5th Ed. Springer Verlag, Germany.
- Hofmann, E.L., 1992. Instrumental neutron activation in geoanalysis. *Journal of Geochemical Exploration* 44, 297–319.
- Jacobsen, S.B., Wasserburg, G.J., 1984. Sm–Nd isotopic evolution of chondrites and achondrites, II. *Earth Planetary Science Letters* 67, 137–150.
- Janousek, V., Braithwaite, C.J.R., Bowes, D.R., Gerdes, A., 2004. Magma-mixing in the genesis of Hercynian calc-alkaline granitoids: an integrated petrographic and geochemical study of the Sázava intrusion, Central Bohemian Pluton, Czech Republic. *Lithos* 78, 67–99.
- Krogh, T.E., 1973. A low-contamination method for hydrothermal decomposition of zircon and extraction of U and Pb for isotopic age determination. *Geochemical and Cosmochimica Acta* 48, 505–511.
- Krogh, T.E., 1982. Improved accuracy of U–Pb zircon ages by the creation of more concordant systems using an air abrasion technique. *Geochemical and Cosmochimica Acta* 46, 637–649.
- Lagarde, J.L., Capdevila, R., Fourcade, S., 1992. Granites et collision continentale: l'exemple des granitoides carbonifères dans la chaîne hercynienne ouest-européenne. *Bulletin Société Géologique* 163 (5), 597–610.
- Ludwig, K.R., 2003. *Isoplot 3.00: A Geochronological Toolkit for Microsoft Excel*. Berkeley Geochronology Center, Special Publication n°4.74pp.
- Marques, J.M., Carreira, P.M., Aires-Barros, L., Graça, R.C., 2000. Nature and role of CO<sub>2</sub> in some hot and cold HCO<sub>3</sub>/Na/CO<sub>2</sub>-rich Portuguese mineral waters: a review and reinterpretation. *Environmental Geology* 40 (1,2), 53–63.
- Martins, H.C.B., 1998. Geoquímica e petrogénese de granitoides biotíticos tarditectónicos e pós-tectónicos. Implicações metalogénicas. Ph.D. Thesis. Universidade de Trás-os-Montes e Alto Douro, Vila Real, Portugal.
- Martins, H.C.B., Noronha, F., 2000. Sources of late-Hercynian biotite-rich granite plutons from Northern Portugal: inferences from zircon morphology. *Cadernos Laboratório Xeolóxico de Laxe* 25, 257–260.
- Martins, H.C.B., Almeida, A., Noronha, F., Leterrier, J., 2001. Novos dados geocronológicos de granitos da região do Porto: granito do Porto e granito de Lavadores. In: Boski, Tomasz, et al. (Eds.) *Actas do VI Congresso de Geoquímica dos Países de Língua Portuguesa e XII Semana de Geoquímica*. Universidade do Algarve, Portugal.
- Martins, H.C.B., Sant’Ovaia, H., Noronha, F., 2007. Post-tectonic granite intrusion controlled by a deep Variscan fault in Northern Portugal. *Cadernos Laboratório Xeolóxico de Laxe* 25, 257–260.
- Matte, P., 1991. Accretionary history and crustal evolution of the Variscan Belt in Western Europe. *Tectonophysics* 196, 309–337.
- Mendes, A.C., Dias, G., 2004. Mantle-like Sr–Nd isotope composition of Fe–K subalkaline granites: the Peneda-Gerês Variscan massif (NW Iberian Peninsula). *Terra Nova* 16, 109–115.
- Michard, A., Gurriet, P., Soudant, M., Albarède, F., 1985. Nd isotopes in French Phanerozoic shales: external versus internal aspects of crustal evolution. *Geochemical and Cosmochimica Acta* 49, 601–610.
- Moreno-Ventas, L., Rogers, G., Castro, A., 1995. The role of hybridization in the genesis of Hercynian granitoids in the Gredos Massif, Spain: inferences from Sr–Nd isotopes. *Contributions to Mineralogy and Petrology* 120, 137–149.
- Neiva, A.M., Gomes, M.E.P., 1991. Geochemistry of the granitoid rocks and their minerals from Lixa do Alvão-Alfarela de Jales-Toureninho (Vila Pouca de Aguiar, northern Portugal). *Chemical Geology* 89, 305–327.
- Noronha, F., Leterrier, J., 2000. Complexo metamórfico da foz do Douro (Porto). *Geoquímica e geocronologia*. *Revista Real Academia Galega de Ciências* 19, 21–42.
- Noronha, F., Ramos, J.M.F., Rebelo, J.A., Ribeiro, A., Ribeiro, M.L., 1979. Essai de corrélation des phases de déformation hercynienne dans le Nord-Ouest Péninsulaire. *Boletim da Sociedade Geológica de Portugal* 21, 227–237.
- Orsini, J.B., Cocirca, C., Zorpi, M.J., 1991. Genesis of mafic microgranular enclaves through differentiation of basic magmas, mingling and chemical exchanges with their host granitoid magmas. In: Didier, J., Barbarin, B. (Eds.), *Enclaves and Granite Petrology*. Developments in Petrology, vol. 13. Elsevier, Amsterdam.
- Paquette, J.L., Ménot, R.P., Pin, C., Orsini, J.B., 2003. Episodic and short-lived granitic pulses in a post-collisional setting: evidence from precise U–Pb zircon dating through a crustal cross-section in Corsica. *Chemical Geology* 198, 1–20.
- Parrish, R.R., 1987. An improved micro-capsule for zircon dissolution in U–Pb geochronology. *Chemical Geology* 66, 99–102.
- Pichavant, M., Montel, J.M., Richard, L.R., 1992. Apatite solubility in peraluminous liquids: experimental data and extension of the Harrison–Watson model. *Geochemical and Cosmochimica Acta* 56, 3855–3861.
- Pin, C., Santos Zalduegui, J.F., 1997. Sequential separation of light rare earth elements, thorium and uranium by miniaturized extraction chromatography: application to isotopic analyses of silicate rocks. *Analytical Chimica Acta* 339, 79–89.
- Pin, C., Briot, D., Bassin, C., Poitras, F., 1994. Concomitant separation of strontium and samarium–neodymium for isotopic analyses in silicate samples, based on specific extraction chromatography. *Analytical Chimica Acta* 298, 209–217.
- Pinto, M.S., Casquet, C., Ibarrola, E., Corretgé, L.G., Ferreira, M.P., 1987. Síntese geocronológica dos granitoides do Macizo Hespérico. In: Bea, F., Carmina, A., Gonzalo, J.C., Plaza, M.L., Rodrigues, J.M.L. (Eds.), *Geología de los granitoides y rocas asociadas del Macizo Hespérico*. Editorial Rueda, Madrid (Libro Homenaje a L.C.G. Figurella).
- Pupin, J.P., 1980. Zircon and granite petrology. *Contributions to Mineralogy and Petrology* 110, 463–472.
- Renna, M.R., Tribuzio, R., Tiepolo, M., 2006. Interaction between basic and acid magmas during the latest stages of the post-collisional Variscan evolution: Clues from the gabbro-granite association of Ota (Corsica-Sardinia batholith). *Lithos* 90, 92–110.
- Ribeiro, A., 1974. Contribution à l’étude tectonique de Trás-os-Montes Oriental. *Comunicações dos Serviços Geológicos de Portugal* 24, 1–168.
- Ribeiro, M.A., 1998. Estudo litogeoquímico das formações metassedimentares encaixantes de mineralizações em Trás-os-Montes Ocidental. Implicações metalogénicas. Ph.D. Thesis. Universidade do Porto, Portugal.
- Ribeiro, A., Pereira, E., Dias, R., 1990. Structure in the Iberian Peninsula. In: Dallmeyer, R.D., Martinez Garcia (Eds.), *Pre-Mesozoic Geology of Iberia*. Springer-Verlag, Berlin, pp. 220–236.
- Ribeiro, M.A., Sant’Ovaia, H., Martins, H.C.B., Ramos, R., Noronha, F., 2004. Tectono-stratigraphic and structural control on the late-Variscan plutonism and metamorphism in an Iberian crustal segment (Northern Portugal): ranging from megascale to micro-scale. In: *Abstracts (CD-ROM) of the 32<sup>nd</sup> International Geological Congress*, Florence, Italy.
- Rochette, P., 1987. Magnetic susceptibility of the rock matrix related to magnetic fabric studies. *Journal of Structural Geology* 9 (8), 1015–1020.
- Saint Blanquet, M., (Unpublished). EXAMS, an Excell macro for automatic computing of AMS data. Université de Toulouse.
- Sant’Ovaia, H., 2000. O maciço granítico pós-tectónico de Vila Pouca de Aguiar: estudo petro-estrutural e mecanismo de instalação. Ph.D. Thesis. Universidade do Porto / Université Paul Sabatier, Toulouse.
- Sant’Ovaia, H., Noronha, F., 2005a. Classificação de granitos hercínicos com base nas suas características petrográficas. *Cadernos Laboratório Xeolóxico de Laxe* 30, 87–98.
- Sant’Ovaia, H., Noronha, F., 2005b. Gravimetric anomaly modelling of the post-tectonic granite pluton of Águas Frias-Chaves (Northern Portugal). *Cadernos Laboratório Xeolóxico de Laxe* 30, 75–86.
- Sant’Ovaia, H., Bouchez, J.L., Noronha, F., Leblanc, D., Vigneresse, J.L., 2000. Composite-laccolith emplacement of the post-tectonic Vila Pouca de Aguiar granite pluton (northern Portugal): a combined AMS and gravity study. *Transactions of the Royal Society of Edinburgh Earth Science* 91, 123–137.
- Schaltegger, U., Corfu, F., 1992. The age and source of late Hercynian magmatism in the central Alps: evidence from precise U–Pb ages and initial Hf isotopes. *Contributions to Mineralogy and Petrology* 111, 329–344.

- Silva, M.M.V., Neiva, A., 2004. Geochemistry of high-Mg-K microgranular enclaves and host granites from Vila Nova de Gaia, Northern Portugal. In: Abstracts (CD-ROM) of the 32<sup>nd</sup> International Geological Congress, Florence, Italy.
- Slaby, E., Martin, E., 2008. Mafic and felsic magma interaction in granites: the Hercynian Karkonosze Pluton (Sudetes, Bohemian Massif). *Journal of Petrology* 49, 353–391.
- Stacey, J.S., Kramers, J.D., 1975. Approximation of terrestrial lead isotope evolution by a two-stage model. *Earth and Planetary Science Letters* 26, 207–221.
- Steiger, R.H., Jäger, E., 1977. Subcommittee on geochronology: convention in the use of decay constants in geo- and cosmochemistry. *Earth and Planetary Science Letters* 36, 359–362.
- Vernon, R.H., 1984. Microgranitoid enclaves in granites: globules of hybrid magma quenched in a plutonic environment. *Nature* 309, 438–439.
- Vigneresses, J.L., 1990. Use and misuse of geophysical data to determine the shape at depth of granitic intrusions. *Geological Journal* 25, 249–260.
- Vigneresses, J.L., Cannat, M., 1987. Mesure des paramètres physiques dans le sondage d'Echassières (vitesse sismique, porosité, densité). *Géologie de la France, BRGM* 2 (3), 145–148.
- Villaseca, C., Herreros, V., 2000. A sustained felsic magmatic system: the Hercynian granitic batholith of the Spanish Central System. *Transactions of Royal Society of Edinburgh Earth Science* 91, 207–219.
- Villaseca, C., Barbero, L., Herreros, V., 1998a. A re-examination of the typology of peraluminous granite types in intracontinental orogenic belts. *Transactions of the Royal Society of Edinburgh Earth Science* 89, 113–119.
- Villaseca, C., Barbero, L., Rogers, G., 1998b. Crustal origin of Hercynian peraluminous granitic batholiths of central Spain: petrological, geochemical and isotopic (Sr–Nd) arguments. *Lithos* 43, 55–79.
- Villaseca, C., Downes, H., Pin, C., Barbero, L., 1999. Nature and composition of the lower continental crust in central Spain and the granulite–granite linkage: inferences from granulitic xenoliths. *Journal of Petrology* 40 (1), 465–496.
- Watson, E.B., Harrison, T.M., 1984. Accessory minerals and the geochemical evolution of crustal magmatic systems: a summary and prospectus of experimental approaches. *Physics of the Earth and Planetary Interiors* 35, 19–30.
- Wedepohl, K.H., 1995. The composition of the continental crust. *Geochimica and Cosmochimica Acta* 59, 1217–1232.